ESC European Society of Cardiology
European Heart Journal (2025) **00**, 1–17
https://doi.org/10.1093/eurheartj/ehaf694

FASTTRACK - CLINICAL RESEARCH
Vascular biology and medicine

Reticulated platelets in coronary artery disease: a multidimensional approach unveils prothrombotic signalling and novel therapeutic targets

Kilian Kirmes [1,2,†], Jiaying Han [1,2,†], Melissa Klug[1,2,3,†], Conor J. Bloxham [1,4,†], Olena Babyak[4], Judith Bernett [3], Lis Arend [3], Quirin Manz [3], Leonora Raka[3,4], Leon Schwartz[3], Markus Hoffmann [3,5], Marc Rosenbaum[6,7], Jürgen Ruland[6,7], Octavia-Andreea Ciora[3], Zakaria Louadi[8], Olga Tsoy[8], Khalique Newaz [8], Jessica Modica[9,10], Carola Conca Dioguardi[10,11], Clelia Peano[10,11], Michaela Müller[3], Donato Santovito[2,12], Giacomo Viggiani[1], Stephanie Kühne[4], Moritz von Scheidt [2], Leo Nicolai[2,13], Tianjiao Wu[13], Jan Baumbach [8], Mauro Chiarito[9], Karl-Ludwig Laugwitz[1,2], Gianluigi Condorelli[9], Philip W.J. Raake[4], Markus List[3,14], Isabell Bernlochner[1,2], and Dario Bongiovanni [4,9,*]

[1]Department of Internal Medicine I, University Hospital Rechts der Isar, Technical University of Munich, Munich, Germany; [2]German Center for Cardiovascular Research (DZHK), Partner Site Munich Heart Alliance, Munich, Germany; [3]Data Science in Systems Biology, TUM School of Life Sciences, Technical University of Munich, Freising, Germany; [4]Department of Internal Medicine I, University Hospital of Augsburg, Faculty of Medicine, University of Augsburg, Stenglinstraße 2, Augsburg 86156, Germany; [5]National Institute of Diabetes and Digestive and Kidney Diseases, National Institutes of Health, Bethesda, MD, USA; [6]Institute of Clinical Chemistry and Pathobiochemistry, Technical University of Munich, Munich, Germany; [7]TranslaTUM, Center for Translational Cancer Research, Technical University of Munich, Munich, Germany; [8]Institute for Computational Systems Biology, University of Hamburg, Hamburg, Germany; [9]Department of Cardiovascular Medicine, Humanitas Clinical and Research Center IRCCS and Humanitas University, via Alessandro Manzoni 56, 20089 Rozzano, Milan, Italy; [10]Institute of Genetics and Biomedical Research, UoS of Milan, National Research Council, Milan, Italy; [11]National Facility for Genomics, Human Technopole, Via Rita Levi Montalcini 1, Milan, Italy; [12]Institute for Cardiovascular Prevention (IPEK), Ludwig Maximilian University (LMU) of Munich, Munich, Germany; [13]Department of Medicine I, Ludwig Maximilian University Hospital, Ludwig Maximilian University Munich, Munich, Germany; and [14]Munich Data Science Institute (MDSI), Technical University of Munich, Garching, Germany

Received 20 August 2025; accepted 20 August 2025

See the editorial comment for this article 'The silent saboteurs: reticulated platelets in coronary artery disease', by H.E. Park and S.J. Cameron, https://doi.org/10.1093/eurheartj/ehaf656.

Abstract

Background and Aims Reticulated platelets (RPs), hyperreactive and RNA-rich, are associated with increased risk of cardiovascular events and sub-optimal response to antiplatelet therapy in coronary artery disease (CAD). However, the underlying mechanisms remain poorly defined. This study aimed to characterize the molecular and functional phenotype of RPs in CAD and assess their potential as therapeutic targets.

Methods RPs and mature platelets (MPs) were isolated from CAD patients based on RNA content and CD41 expression. Paired RP vs MP comparisons were conducted within each donor. Transcriptomic profiling (RNA-seq) was integrated with high-dimensional proteomics (mass cytometry) and validated in independent cohorts. Functional studies, including flow cytometry-based platelet–platelet binding, *in vitro* thrombosis, platelet spreading, and intracellular phospho-protein profiling, assessed the impact of PI3K and GPVI pathways. Results were curated in *Platlas*, an open-access interactive web resource.

* Corresponding author. Tel: +49 821400168849, Email: dario.bongiovanni@med.uni-augsburg.de
† These authors contributed equally to the study.
© The Author(s) 2025. Published by Oxford University Press on behalf of the European Society of Cardiology. All rights reserved. For commercial re-use, please contact reprints@oup.com for reprints and translation rights for reprints. All other permissions can be obtained through our RightsLink service via the Permissions link on the article page on our site—for further information please contact journals.permissions@oup.com.

Downloaded from https://academic.oup.com/eurheartj/advance-article/doi/10.1093/eurheartj/ehaf694/8244414 by guest on 09 November 2025

Results Among 95 CAD patients, RPs exhibited elevated activation marker expression and enrichment of prothrombotic pathways compared with MPs. RNA-seq revealed upregulation of GP6, TBXA2R, and VWF transcripts, novel GPVI splicing, and RP-specific non-coding RNAs including novel circRNAs. Proteomic and functional assays confirmed heightened PI3K and GPVI signalling, with increased phosphorylation of AKT, PI3K, and SYK, and elevated reactive oxygen species production. RPs showed increased aggregation, spreading and greater recruitment in thrombus formation, which were significantly reduced by PI3K (LY294002) and GPVI (glenzocimab) inhibition.

Conclusions This study provides the first mechanistic explanation for RP hyperreactivity, revealing a distinct molecular profile and identifying GPVI and PI3K inhibition as promising targets for tailored antiplatelet therapy in CAD patients with elevated RPs.

Structured Graphical Abstract

Key Question

Why do patients with high reticulated platelet (RP) levels remain at increased thrombotic risk, despite optimal antiplatelet therapy? What are the underlying molecular mechanisms that could inform more effective, personalised treatment strategies?

Key Finding

RPs displayed a distinct prothrombotic profile with enhanced GPVI and PI3K signalling, elevated activation markers, and unique non-coding RNA signatures. Functional assays confirmed heightened aggregation and thrombus formation, which were attenuated by PI3K and GPVI inhibition.

Take Home Message

Mechanistic profiling reveals that RPs actively contribute to thrombosis through targetable pathways. PI3K and GPVI inhibition may reduce residual thrombotic risk in coronary artery disease patients with elevated RPs, paving the way for precision antiplatelet therapy.

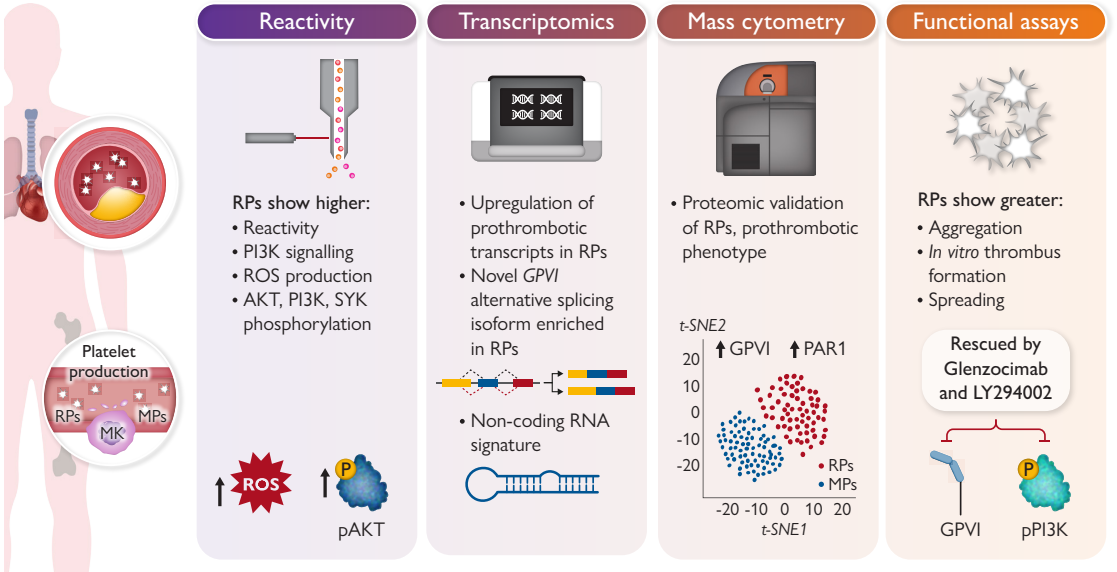

RPs display enhanced reactivity, increased PI3K signalling, ROS production, and phosphorylation of AKT, PI3K, and SYK, contributing to a prothrombotic phenotype. Transcriptomic profiling identified upregulation of prothrombotic transcripts, a novel GPVI isoform, and distinct non-coding RNA signatures in RPs. Mass cytometry confirmed the prothrombotic phenotype of RPs. Functional assays demonstrate increased RP aggregation, spreading, and thrombus formation, which are attenuated by pharmacological inhibition of GPVI (glenzocimab) and PI3K (LY294002). These findings provide the first mechanistic insights to support personalized antiplatelet strategies in high-risk CAD patients with elevated RPs

AKT, Akt kinase/protein kinase B; **CAD**, coronary artery disease; **GPVI**, glycoprotein VI; **MK**, megakaryocyte; **MPs**, mature platelets; **PAR1**, protease-activated receptor 1; **PI3K**, phosphoinositide 3-kinase; **ROS**, reactive oxygen species; **RPs**, reticulated platelets; **SYK**, spleen tyrosine kinase

Kirmes K, *et al. European Heart Journal.*

RPs display enhanced reactivity, increased PI3K signalling, ROS production, and phosphorylation of AKT, PI3K, and SYK, contributing to a prothrombotic phenotype. Transcriptomic profiling identified upregulation of prothrombotic transcripts, a novel GPVI isoform, and distinct non-coding RNA signatures in RPs. Mass cytometry confirmed the prothrombotic phenotype of RPs. Functional assays demonstrate increased RP aggregation, spreading, and thrombus formation, which are attenuated by pharmacological inhibition of GPVI (glenzocimab) and PI3K (LY294002). These findings provide the first mechanistic insights to support personalized antiplatelet strategies in high-risk CAD patients with elevated RPs AKT, Akt kinase/protein

Downloaded from https://academic.oup.com/eurheartj/advance-article/doi/10.1093/eurheartj/ehaf694/8244414 by guest on 09 November 2025

kinase B; CAD, coronary artery disease; GPVI, glycoprotein VI; MK, megakaryocyte; MPs, mature platelets; PAR1, protease-activated receptor 1; PI3K, phosphoinositide 3-kinase; ROS, reactive oxygen species; RPs, reticulated platelets; SYK, spleen tyrosine kinase.

Keywords Coronary artery disease • Reticulated platelets • Thrombocytes • Transcriptomics • Mass cytometry • GPVI

Translational perspective

Despite optimal therapy, coronary artery disease (CAD) patients with elevated reticulated platelets remain at high risk of ischaemic events, highlighting the urgent need for personalized therapeutic strategies. This study provides the first mechanistic explanation of reticulated platelet hyperreactivity, identifying distinct prothrombotic profiles, including GPVI upregulation, PI3K pathway activation, and unique non-coding RNA signatures. Inhibition of PI3K and GPVI reduced reticulated platelets hyperreactivity in experimental settings, offering a promising therapeutic strategy. These findings provide a scientific foundation for the development of personalized strategies aimed at reducing thrombotic risk and improving outcomes in high-risk CAD patients with elevated reticulated platelets through GPVI/PI3K inhibitors.

Introduction

Once considered exclusively involved in vascular haemostasis, platelets have recently been shown to participate in a variety of physiological and pathophysiological processes, including inflammation, immune response, and even tumour progression[1–6]. Platelets exhibit significant heterogeneity in terms of RNA and granule content, size, and expression of transmembrane proteins[7–13]. Additionally, they have been reported to exchange RNA with other vascular cells and engage in complex interactions with immune cells.[14–17] Megakaryocytes contribute to platelet heterogeneity by differentially sorting mRNA and proteins into platelets during thrombopoiesis.[18] Platelet ageing alters RNA content and expression due to the lack of a nucleus and inability to synthesize new mRNA. Nevertheless, platelets retain protein biosynthesis machinery, regulated by activation and pathological conditions.[19] Seminal studies have demonstrated the key role of platelet profiling in the progression of coronary artery disease (CAD),[20,21] supporting further investigations.

Platelet heterogeneity has recently become a focus of pre-clinical and clinical research. To date, the only extensively studied platelet subset is that of immature, reticulated platelets (RPs).[22] These newly released,[23] hyperreactive, RNA-rich platelets are larger and express higher levels of activation markers and adhesion proteins than mature platelets (MPs).[13] RPs also play a more active role in thrombus formation,[24,25] and contain more dense- and α-granules.[12]

RPs can be measured from peripheral blood using point-of-care systems. Their absolute number or fraction has been shown to increase in high-risk populations such as smokers and diabetics, as well as after acute events such as myocardial infarction, surgery, and sepsis.[26–31] Moreover, elevated RPs are associated with an inadequate response to antiplatelet therapy and predict major adverse cardiovascular events in several conditions, including CAD.[32,33] In a recent large randomized trial, we demonstrated that elevated RPs are strong predictors of ischaemic adverse events in patients with acute coronary syndromes treated with optimal antiplatelet therapy, specifically with potent $P2Y_{12}$ inhibitors.[34] This was further validated in a meta-analysis of CAD patients.[35,36] Collectively, these clinical findings indicate that patients with elevated RPs, which represent a relevant number of patients with CAD, remain at high risk for ischaemic events despite optimal antiplatelet therapy, and may benefit from tailored platelet inhibition strategies to reduce this risk. However, the precise biological mechanisms underlying RPs and their association with adverse cardiovascular outcomes have not been fully elucidated, hindering the identification of a clear therapeutic target.

Our early investigations of the RP transcriptome in healthy donors revealed a prothrombotic profile, marked by up-regulated genes encoding key transmembrane receptors.[37] A subsequent study confirmed these findings and revealed distinct structural differences in RPs, including more dense- and α-granules and mitochondria.[12] However, a thorough investigation of RP biology, particularly in patients with CAD, is still lacking. Here, we present a comprehensive multidimensional characterization of RP biology in CAD patients, incorporating in-depth transcriptomics and mass cytometry.

Methods

Reagents, chemicals, equipment, and antibodies are listed in Supplementary data online, *Tables S1* and *S2*.

Study design

CAD patients presenting for clinical follow-up in three German and one Italian university hospitals (Klinikum rechts der Isar, Technical University of Munich; University Hospital of Augsburg, Ludwig Maximilians University Hospital of Munich, Germany and Humanitas University, Rozzano, Milan, Italy) were included in our study (for baseline characteristics see *Table 1* and Supplementary data online, *Table S3*). Exclusion criteria were thrombocytopenia (<100 G/L), thrombocytosis (>500 G/L), and other haematological diseases. This study was approved by the local ethics committees, all participants provided written informed consent, and the study was performed in accordance with the Declaration of Helsinki. Due to the exploratory nature of the study, no formal sample size calculation was performed. However, paired within-donor comparisons ensured analytical robustness across assays. For all transcriptomic, proteomic, and functional analyses, RPs and MPs were identified and compared in a pairwise fashion within the same patient. This intra-individual design eliminates between-patient variability and ensures that each subject serves as their own control, thereby minimizing confounding by clinical factors such as age, sex, comorbidities, or antiplatelet therapy.

Blood sampling and platelet preparation

Peripheral venous blood (12–15 ml) was collected from patients in citrate tubes and immediately processed for downstream analysis. Platelet-rich plasma (PRP) was obtained by centrifugation, as previously described (see Supplementary Methods).[13]

Downloaded from https://academic.oup.com/eurheartj/advance-article/doi/10.1093/eurheartj/ehaf694/8244414 by guest on 09 November 2025

Table 1 Baseline characteristics of the study cohort

Characteristics	All N = 95
Age (years), median (IQR: Q1-Q3)	68.5 [58.7–79.0]
18–39 years, no. (%)	0 (0)
40–64 years, no. (%)	27 (28.4)
65+ years, no. (%)	68 (71.6)
Male sex, no. (%)	70 (73.7)
single antiplatelet therapy, no. (%)	8 (8.4)
dual antiplatelet therapy, no. (%)	85 (89.5)
Thrombocytes (platelets/L), mean (±SD)	223.3 (68.5)
Previous MI, no. (%)	65 (68.4)
Previous PCI, no. (%)	89 (93.7)
Diabetes mellitus, no. (%)	30 (31.6)
Peripheral artery disease, no. (%)	20 (21.1)
Obesity (BMI > 30 kg/m^2), no. (%)	21 (22.1)
Nicotine abuse active, no. (%)	22 (23.2)
Nicotine abuse former, no. (%)	27 (28.4)
Days since last PCI, median (IQR: Q1-Q3)	163.0 [56.5–184.5]

BMI, body mass index; IQR, interquartile range, MI: myocardial infarction, PCI, percutaneous coronary intervention.

Flow cytometry and RP detection

Flow cytometry was performed using the Beckman Coulter Gallios, and cell sorting on the BD FACS Aria III. FCS files were exported and analysed in Kaluza (Beckman Coulter). After doublet exclusion, RPs were identified as the top 15% of Thiazole Orange (TO) intensity, and MPs as the bottom 30%, following established protocols.[13] Platelet reactivity assays and further FACS analysis are described in the Supplementary Methods.

Platelet staining and isolation for RNA sequencing

Platelets were stained, sorted, and isolated using magnetic columns as previously described.[13] Briefly, 300 µl of PRP was stained with 600 µl TO (2:1 v/v), CD41 (1:200 v/v), and DNA Vybrant dye (1:500) to select for platelets (CD41+/DNA−), and avoid leucocyte contamination according to current consensus[38] (*Figure 1A*). Additionally, cells were stained with CD61 magnetic MicroBeads (Miltenyi Biotec) for 10 min. Platelets were then sorted based on their TO signal to isolate the RP and MP populations, as previously described.[13] After sorting, cells were magnetically enriched, and RNA was extracted, eluted in 20 µl of RNase-free water and stored at −80°C. Library preparation and RNA sequencing are described in the Supplementary Methods.

Mass cytometry (CyTOF)

Mass cytometry of PRP was performed as previously described and validated.[39] Six antibodies (CD42a, CD62P, GPVI, PAR1, PEAR1, GPIIb IIIa/αIIbβ3) were custom-conjugated using the MaxPAR X8 antibody conjugation kit (Fluidigm Sciences) following the manufacturer's protocol. All other 15 antibodies were purchased pre-conjugated. A full list of antibodies and reagents is provided in Supplementary data online, *Tables S1* and *S2*.

After PRP preparation, the samples were stained with the antibody cocktail. For each donor, one baseline and one TRAP-stimulated (10 µM) sample were prepared, as previously described (see Supplementary method).[39] To exclusively select platelets and avoid possible leucocyte contamination, only CD45 negative and CD41 (GPIIb) and CD61 (GPIIIa) positive events were considered, using a previously described gating strategy (see Supplementary data online, *Figure S1*).[39] To detect RPs and MPs, platelets with the highest 15% 191Ir and 193Ir signals [nucleic acid intercalators, part of cytometry by time of flight/mass cytometry (CyTOF) pipeline] were gated as the RP population, while platelets with the lowest 30% 191Ir and 193Ir signals were gated as MPs.

Functional validations, computational and statistical analyses are described in the Supplementary Methods.

Results

Study cohort

A total of 95 CAD patients with history of previous percutaneous coronary intervention (PCI) were enrolled. Given the complexity of the experimental procedures, requiring extensive sample preparation, subgroups of patients were assigned to transcriptomics, proteomics, or downstream signalling assays, as these could not be conducted simultaneously. Specifically, 19 patients were included in the FACS reactivity assays, 19 patients in the transcriptomic analyses (one was excluded after quality control) and 11 patients in mass cytometry. Additionally, 46 CAD patients were used for validation assays using droplet digital polymerase chain reaction (ddPCR) and signalling analysis. The median age of the cohort was 68.5 years, with 73.7% of the patients being male. 68.4% had a history of myocardial infarction, 31.6% had diabetes, and 23.2% were active smokers. Most patients (89.5%) were on dual antiplatelet therapy following PCI (median time since last PCI: 165 days). Detailed baseline characteristics of these populations are provided in Supplementary data online, *Table S3*.

Reticulated platelets display high *ex vivo* hyper-reactivity

We assessed the reactivity profiles of MP and RP populations in patients with CAD using FACS. At baseline, RPs exhibited significantly higher expression of the activation marker P-selectin (CD62P) compared with MPs (*Figure 1* and Supplementary data online, *Table S4*). This difference became even more pronounced following stimulation with TRAP, adenosine 5′-diphosphate (ADP), and collagen-related peptide (CRP), where RPs consistently showed significantly higher CD62P expression (*Figure 1B–D*). To confirm cell viability and reactivity post-sorting, we ensured that platelet reactivity was preserved, validating our ability to isolate the hyper-reactive RP subgroup. After stimulation, RPs continued to exhibit significantly higher expression of CD62P compared with MPs (see Supplementary data online, *Figure S2*).

RNA sequencing

As expected, the total amount of RNA extracted from platelets after sorting was significantly higher in RPs compared with MPs (median difference 952pg RNA/sample [95% confidence interval (CI) 400, 1536] $P = .0001$, further details in Supplementary data online, *Table S5*). After quality control, including evaluation of leucocyte marker expression (see Supplementary data online, *Figure S3*), data analysis using a cut-off of normalized counts of one across the 38 samples (RPs and MPs from 19 donors), we detected 14 582 transcripts. Of these, 76.5% were protein-coding transcripts, 7.59% were pseudogenes, and

Downloaded from https://academic.oup.com/eurheartj/advance-article/doi/10.1093/eurheartj/ehaf694/8244414 by guest on 09 November 2025

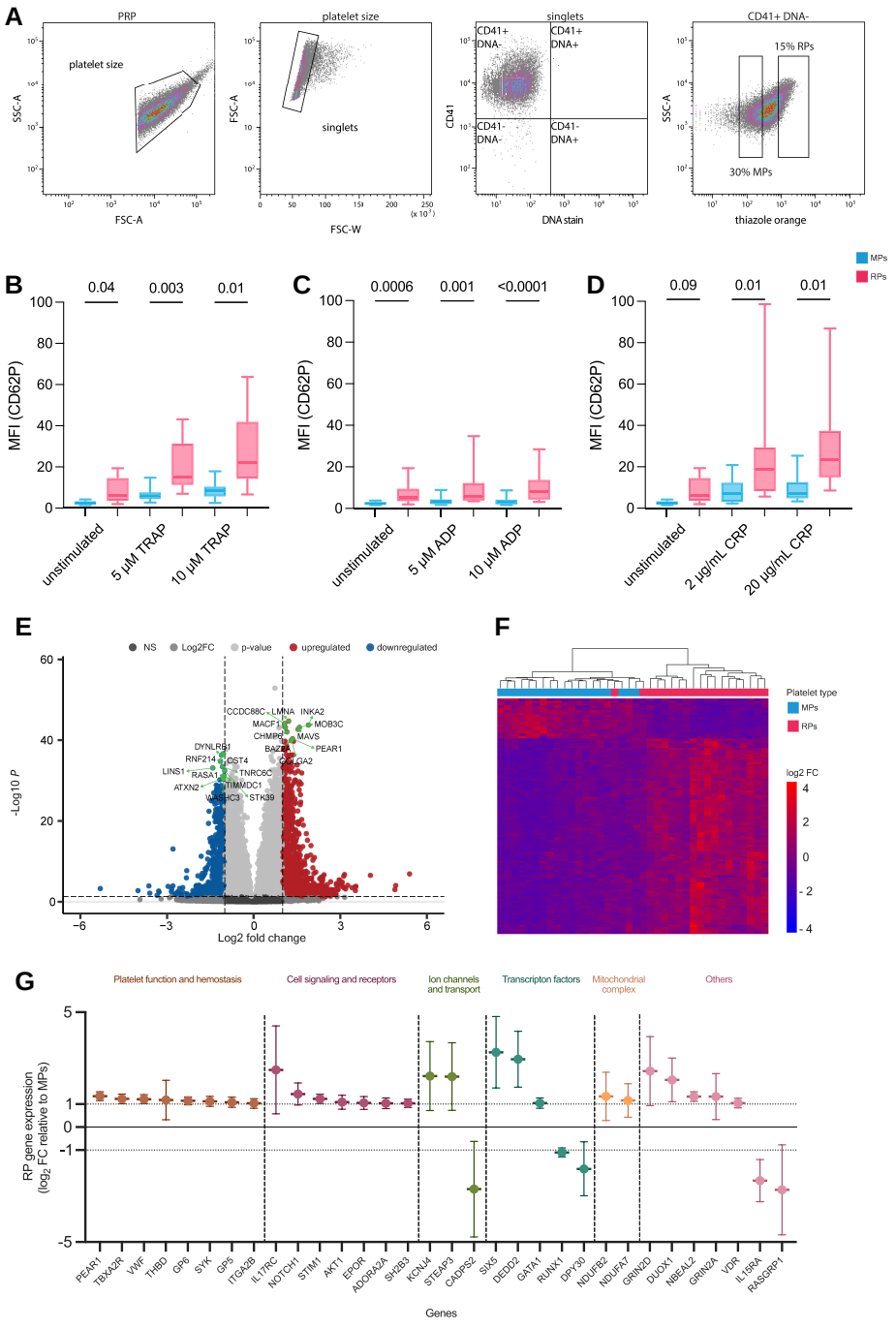

Figure 1 Elevated reactivity and differential gene expression in reticulated platelets. (*A*) Flow cytometry gating strategy. First, the gate is applied to stained platelet-rich plasma (PRP) separating the platelets by size using FSC/SSC. Then, doublets are excluded by a high FSC-width. Afterwards, platelets are sorted after CD41 (BV: 421 nm) and DNA staining (Vybrant DyeCycle Ruby Stain: 638 nm) for platelet isolation and leucocyte to prevent leucocyte contamination. Next, platelets are gated for RNA^{low} platelets (mature platelets, MPs) and RNA^{high} platelets (reticulated platelets, RPs). Platelets with the highest 15% TO signal are defined as RPs, platelets with the lowest 30% TO signal as MPs (TO: 488–550 nm). (*B–D*) CD62P expression of MPs and RPs after TRAP (5 or 10 µM; *B*), ADP (5 or 10 µM; *C*) or CRP stimulation (2 or 20 µg/ml; *D*). RPs showed significantly higher expression of the activation marker P-selectin at rest and after activation ($N = 15$). (*E*) Volcano plot showing significantly up-regulated (red) and down-regulated (blue) transcripts in RPs. (*F*) Heatmap illustrates the top 100 DEGs using a negative binomial linear model via the DESeq2 pipeline. Each row in the heatmap represents the log-ratio intensity data of a single DEG, with expression levels depicted as a gradient from low (blue) to high (red). (*G*) Expression levels of biologically relevant, differentially regulated genes. ($N = 19$). ADP, adenosine 5′-diphosphate; CD62P, P-Selectin; CRP, collagen-related peptide; DEG, differentially expressed gene; MFI, mean fluorescence intensity; MPs, mature platelets; RPs, reticulated platelets; TRAP, thrombin receptor activation peptide.

Downloaded from https://academic.oup.com/eurheartj/advance-article/doi/10.1093/eurheartj/ehaf694/8244414 by guest on 09 November 2025

15.86% were other non-coding genes (see Supplementary data online, *Figure S4*). Among these transcripts, 2213 genes were differentially regulated, with 1531 genes up-regulated in RPs and 682 down-regulated (*Figure 1E–G*). The comprehensive list of differentially expressed genes (DEGs) is available in Supplementary data online, *Table S6* including $\log_2$ fold changes, *P*-values and 95% confidence intervals.

Numerous transcripts encoding surface proteins involved in platelet activation were significantly up-regulated in RPs. These include glycoproteins *GPV* (1.08 $\log_2$FC), *GPVI* (1.14 $\log_2$FC), and their downstream target *SYK* (1.12 $\log_2$FC), as well as G protein-coupled receptors such as adrenoceptor *ADRA2A* (1.04 $\log_2$FC), thrombin receptor *PAR4* (F2RL3, 1.16 $\log_2$FC), thromboxane A2 receptor (*TBXA2R*, 1.23 $\log_2$FC), and purinergic receptor *P2RX1* (1.20 $\log_2$FC). Moreover, an array of integrin and adhesion molecule transcripts were also significantly up-regulated in RPs, including integrins α2b (*GPIIb*, part of the fibrinogen receptor, *ITGA2B*, 1.03 $\log_2$FC), *ITGA5* (1.13 $\log_2$FC), *ICAM5* (1.70 $\log_2$-FC), and the platelet aggregation receptor *PEAR1* (1.34 $\log_2$FC). Furthermore, von Willebrand factor (*VWF*) transcripts were elevated in RPs (1.22 $\log_2$FC). Notably, the expression of the $P2Y_{12}$ receptor did not differ significantly between RPs and MPs (see Supplementary data online, *Figure S5*).

Amidst the notable enrichment of prothrombotic pathways, prostaglandin I2 receptor *PTGIR* (1.58 $\log_2$FC) emerged as the sole antithrombotic receptor up-regulated in RPs. Additionally, there was an upregulation of the endogenous anti-inflammatory protein annexin A1 (*ANXA1*) (1.53 $\log_2$FC), which can inhibit platelet–monocyte interactions. Major platelet signalling proteins involved in the key PI3K/RAC (Rho family)-alpha serine/threonine-protein kinase (AKT) and calcium signalling pathways were also significantly up-regulated in RPs, including *AKT1* (1.11 $\log_2$FC), *PLCB3* (1.62 $\log_2$FC), and *PLCD3* (1.08 $\log_2$FC).

In RPs, several transcriptional regulators were down-regulated. These included the poly(A)-specific ribonuclease *PARN*, which plays a role in mRNA degradation and noncoding RNA maturation processes; the microRNA (miRNA) regulator TNRC6A, a key component of miRNA repressor complexes; and the splicing factor *LUC7L3* (respectively, −1.06 $\log_2$FC, −1.08 $\log_2$FC, −1.05 $\log_2$FC). Additionally, the transcription factor *RUNX1*, known for its involvement in platelet and bleeding disorders,[40,41] was significantly decreased (−1.10 $\log_2$FC) along with protein kinase N2 *PKN2* (−1.04 $\log_2$FC). A list of biologically relevant differentially regulated genes is provided in *Table 2*.

Gene ontology and functional cluster annotation analyses revealed a significant enrichment of terms associated with platelet function and haemostasis such as 'platelet activation' (GO:0030168) in RPs (*Figure 2*; Supplementary Results; Supplementary data online, *Figure 6*, *Tables S7–S13*). Gene set enrichment analysis (GSEA, *Figure 3*) identified multiple significantly overrepresented categories in RPs related to platelet activity and their functions: *platelet aggregation* (NES = 2.53), *platelet formation* (NES = 2.39), and *platelet activation* (NES = 2.32). We also observed an enrichment in important signalling pathways, including *cytokine-mediated signalling* (NES = 1.62) and *immune response-activating signalling pathways* (NES = 1.50). The entire list of GSEA categories can be found in Supplementary data online, *Table S14*.

Alternative splicing events

We detected 116 differential alternative splicing events in RPs compared with MPs (ΔPSI > 0.2; confidence >0.95, Supplementary data online, *Table S15*). Among these, the collagen receptor GPVI gene (Ensembl ID ENSG00000088053) showed previously unrecognized splicing patterns which differ between RPs and MPs. Using sashimi plots, we visualized the GPVI splicing events and identified the skipping of two novel exons (*Figure 4A*) that are absent from the current genome annotation. These findings suggest the expression of potential novel isoforms incorporating one or both newly identified exons. In RPs (*Figure 4A*, top), the proportion of annotated isoforms (ENST00000417454 and ENST00000310373) relative to the novel ones is higher ($\Psi = +0.33$) compared with MPs (*Figure 4B*, bottom). This result was experimentally validated using ddPCR in an independent cohort of CAD patients (*Figure 4C*) but could not be further validated by immunoblotting, probably due to the low yield of proteins obtained after sorting. Compared to the canonical GPVI isoform (Ensembl transcript ID ENST00000417454), which consists of 339 amino acids, the novel isoforms lack amino acids from positions 222 to 339 (see Supplementary data online, *Figure S7*). Notably, the missing segment includes positions 268 to 287, which are predicted to form transmembrane helices based on the membrane protein topology prediction method TMHMM[42] and further supported by AlphaFold[43] (*Figure 4B*). These findings suggest that the two novel exons may affect critical functional protein domains compared with the canonical *GPVI* isoform and warrant further investigations.

miRNA sequencing

The miRNA sequencing of RPs and MPs from 19 patients identified a total of 270 expressed miRNAs (see Supplementary data online, *Figs S8* and *S9*). Among these, 33 were differentially regulated, with 28 up-regulated in RPs and 5 up-regulated in MPs (*Figure 5A*, Supplementary data online, *Table S16*). Of note, miRNA miR-432 has previously been associated with increased platelet aggregation in patients with stable CAD[44] (*Figure 5B*). Similarly, miRNA miR-409 has been reported to correlate with heart failure in patients with mitral regurgitation,[45] and miR-134 has been identified as a biomarker for acute myocardial infarction and increased mortality.[46] An analysis of putative validated targets of down-regulated miRNAs in RPs, based on miRTar Base, identified 697 functionally interactions. Of these, 24 overlapped with up-regulated transcripts in RPs (see Supplementary data online, *Table S17*). Conversely, analysis of targets for up-regulated miRNAs in RPs revealed 85 functionally interactions, but none corresponded to down-regulated transcripts in RPs.

Circular RNA analysis

A total of 1 710 330 back-splicing events were identified, generating 87 573 distinct circRNAs. After normalization and filtering, 26 197 circRNAs were retained for further analysis (see Supplementary data online, *Figure S10*). RPs exhibited a significantly higher number of normalized circRNAs reads compared with MPs (mean difference 0.37×10^6 reads [95% CI 0.03, 0.72], $P = .03$, *Figure 5C*). Principal component analysis revealed a clear separation between MPs and RPs based on circRNAs expression profiles (*Figure 5D* left). Differential expression analysis identified 2916 circRNAs with significant regulation between RPs and MPs: 1180 were up-regulated in RPs, while 1736 were down-regulated (*Figure 5D* right). Interestingly, three circRNAs were exclusively expressed in RPs and absent in MPs (*Figure 5E*), despite the host genes having comparable mRNA expression levels in both populations (*Figure 5F*). These included circRNA chr2:9350807-9385358 (ASAP2), circRNA chr16:4996854-5003573 (SEC14L5), and circRNA chr12:132508152-132527988 (FBRSL1), which have not yet been described and could serve as potential new markers.

Downloaded from https://academic.oup.com/eurheartj/advance-article/doi/10.1093/eurheartj/ehaf694/8244414 by guest on 09 November 2025

Table 2 Representative list of differentially expressed genes in reticulated platelets

Genes	Description	log_2FC RPs vs MPs	95% CI	*P*-value
ICAM5	Intercellular adhesion molecule 5	1.70	[.86, 2.55]	2.60×10^{-4}
PTGIR	Prostaglandin I2 receptor	1.58	[1.32, 1.85]	2.03×10^{-30}
AKAP8L	A-Kinase Anchor Protein 8-Like	1.56	[1.00, 2.11]	2.09×10^{-07}
ANXA9	Annexin A9	1.53	[.67, 2.39]	1.40×10^{-03}
PEAR1	Platelet endothelial aggregation receptor 1	1.34	[1.15, 1.53]	4.49×10^{-41}
PLXNB2	Plexin B2	1.30	[.94, 1.67]	3.27×10^{-11}
STIM1	Stromal interaction molecule 1	1.23	[1.04, 1.43]	2.61×10^{-33}
TBXA2R	Thromboxane A2 receptor	1.23	[1.02, 1.44]	2.08×10^{-29}
VWF	Von Willebrand factor	1.22	[1.02, 1.41]	3.07×10^{-33}
P2RX1	Purinergic receptor P2 × 1	1.20	[.96, 1.43]	1.38×10^{-21}
F2RL3	Thrombin receptor PAR4	1.16	[.94, 1.38]	1.19×10^{-23}
GPVI	Glycoprotein VI platelet	1.14	[.98, 1.31]	1.30×10^{-38}
ORAI2	Calcium release-activated modulator 2	1.14	[.96, 1.31]	5.79×10^{-35}
ITGA5	Integrin, alpha5	1.13	[.75, 1.52]	4.06×10^{-08}
SYK	Spleen-associated tyrosine kinase	1.12	[.90, 1.33]	2.14×10^{-23}
AKT1	AKT Serine/Threonine Kinase 1	1.09	[.79, 1.38]	3.39×10^{-12}
IL16	Interleukin 16	1.08	[.83, 1.33]	2.16×10^{-16}
GP5	Glycoprotein V platelet	1.08	[.86, 1.29]	6.98×10^{-22}
ADRA2A	Adrenoceptor alpha 2A	1.04	[.82, 1.25]	2.56×10^{-20}
ITGA2B	Integrin, alpha2b (platelet glycoprotein IIb)	1.03	[.83, 1.24]	4.67×10^{-22}
ITGB5	Integrin subunit beta 5	1.01	[.83, 1.19]	2.04×10^{-27}
TLN1	Talin 1	1.01	[.75, 1.26]	1.10×10^{-13}
PKN2	Protein kinase N2	−1.04	[−1.24, −.83]	3.39×10^{-21}
LUC7L3	LUC7 like 3 pre-MRNA Splicing factor	−1.05	[−1.26, −.85]	1.80×10^{-22}
PARN	Poly(A)-specific ribonuclease	−1.06	[−1.29, −.84]	1.33×10^{-19}
TNRC6C	GW182, miRNA regulation	−1.08	[−1.25, −.91]	3.62×10^{-34}
BRIX1	BRX1, biogenesis of ribosomes	−1.34	[−1.82, −.86]	2.13×10^{-07}
EMC2	ER membrane protein complex subunit 2	−1.47	[−1.74, −1.20]	1.03×10^{-25}
NOS1AP	Nitric oxide synthase 1 adaptor protein	−1.49	[−1.85, −1.14]	1.49×10^{-15}

Platlas

We developed an interactive website (https://exbio.wzw.tum.de/platlas) to share our transcriptome dataset and analysis results. The site includes differential expression, enrichment, miRNA, circRNA, and splicing analyses, with customizable filters enabling full reproducibility.

Transcriptome validation by droplet digital PCR

To validate the transcriptomic findings, several differentially regulated transcripts were analysed using ddPCR in an independent cohort of CAD patients. Validation was performed on 20 CAD independent patients, with at least eight different donors included for each gene. Consistent with the sequencing data, ddPCR confirmed the upregulation of *GPVI* [mean difference 1.81 FC (95% CI 1.45, 2.12) $P < .0001$], *F2RL3* [*PAR4*, mean difference 1.10 FC (95% CI 0.9, 2.6), $P = .0005$], and *TBXA2R* [median difference 1.20 FC (95% CI 0.4, 2.5), $P = .0005$] in RPs, while *LUC7C3* [median difference 0.45 FC (95% CI 0.0, 1.7), $P = .02$] and *PKN2* [mean difference 1.27 FC (95% CI .81, 1.72), $P < .0001$] were down-regulated in RPs (*Figure 3D*). Additionally, an upregulation of the AD isoform of *GPVI* in RPs was observed [mean difference 0.41 FC (95% CI .027, .80), $P = .04$, *Figure 4C*].

Downloaded from https://academic.oup.com/eurheartj/advance-article/doi/10.1093/eurheartj/ehaf694/8244414 by guest on 09 November 2025

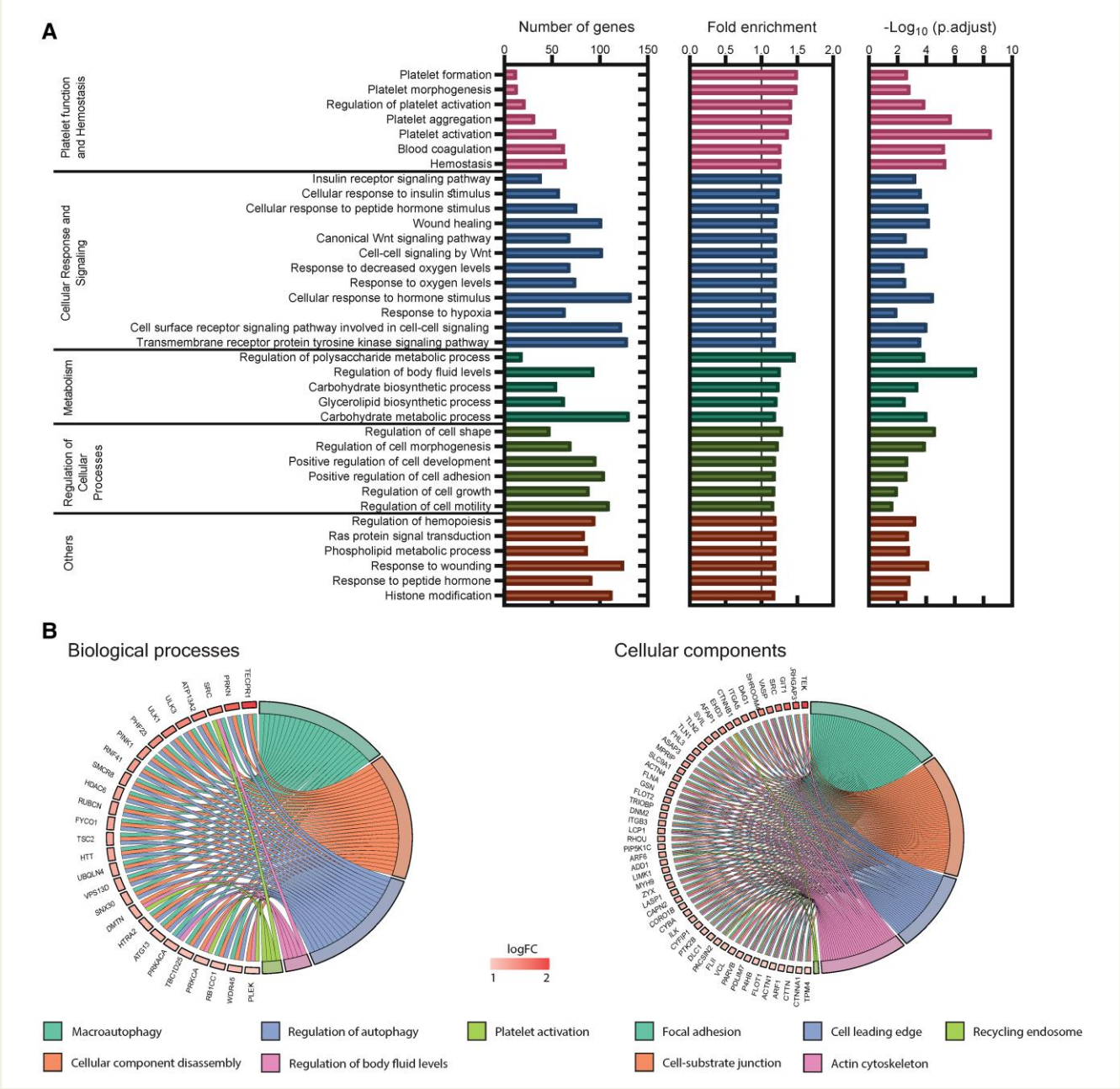

Figure 2 Gene Ontology (GO) analysis of RNA sequencing of RPs compared to MPs. (*A*) GO analysis of biological processes: GO terms associated with biological processes are shown. In RPs significantly enriched GO terms ($P \leq .05$) are shown along with the number of genes associated with each term, their fold enrichment, and the adjusted *P*-value. (*B*) Circular plots depicting fold change of selected overrepresented GO terms in RPs and their corresponding DEGs for biological processes and cellular components ($N = 19$). DEG, differentially expressed gene; GO, gene ontology; MPs, mature platelets; RPs, reticulated platelets

Mass cytometry of platelets

Bioinformatic analysis of mass cytometry revealed a gradient of separation between the two platelet subpopulations, RPs and MPs, highlighting the heterogeneity within the platelet population (*Figure 6A*). Several transmembrane receptors and activation markers were significantly upregulated in RPs compared with MPs (*Figure 6A and B*). Notably, activation markers in non-stimulated platelets were elevated in RPs, including CD62P [median difference 0.27 median signal intensity—MSI (95% CI .13, .64), in RPs and MPs, respectively] and CD63 [median difference 0.38 MSI (95% CI .31, .58)]. Key druggable targets were also upregulated in RPs, such as the collagen receptor GPVI [median difference 0.78 MSI (95% CI .64, .91)], the major thrombin receptor PAR1 [median difference 0.71 MSI (95% CI .54, .93)], the glycoprotein Ib-IX-V complex [CD42a median difference 0.72 MSI (95% CI .26, 1.06) and CD42b median difference 0.53 MSI (95% CI .28, 1.03)], and the integrin α2β1 [CD29 median difference 0.75 MSI (95% CI .55, .92)] (*Figure 6C*, Supplementary data online, *Tables S18* and *S19*). RPs consistently displayed higher expression of platelet activation markers, including

Downloaded from https://academic.oup.com/eurheartj/advance-article/doi/10.1093/eurheartj/ehaf694/8244414 by guest on 09 November 2025

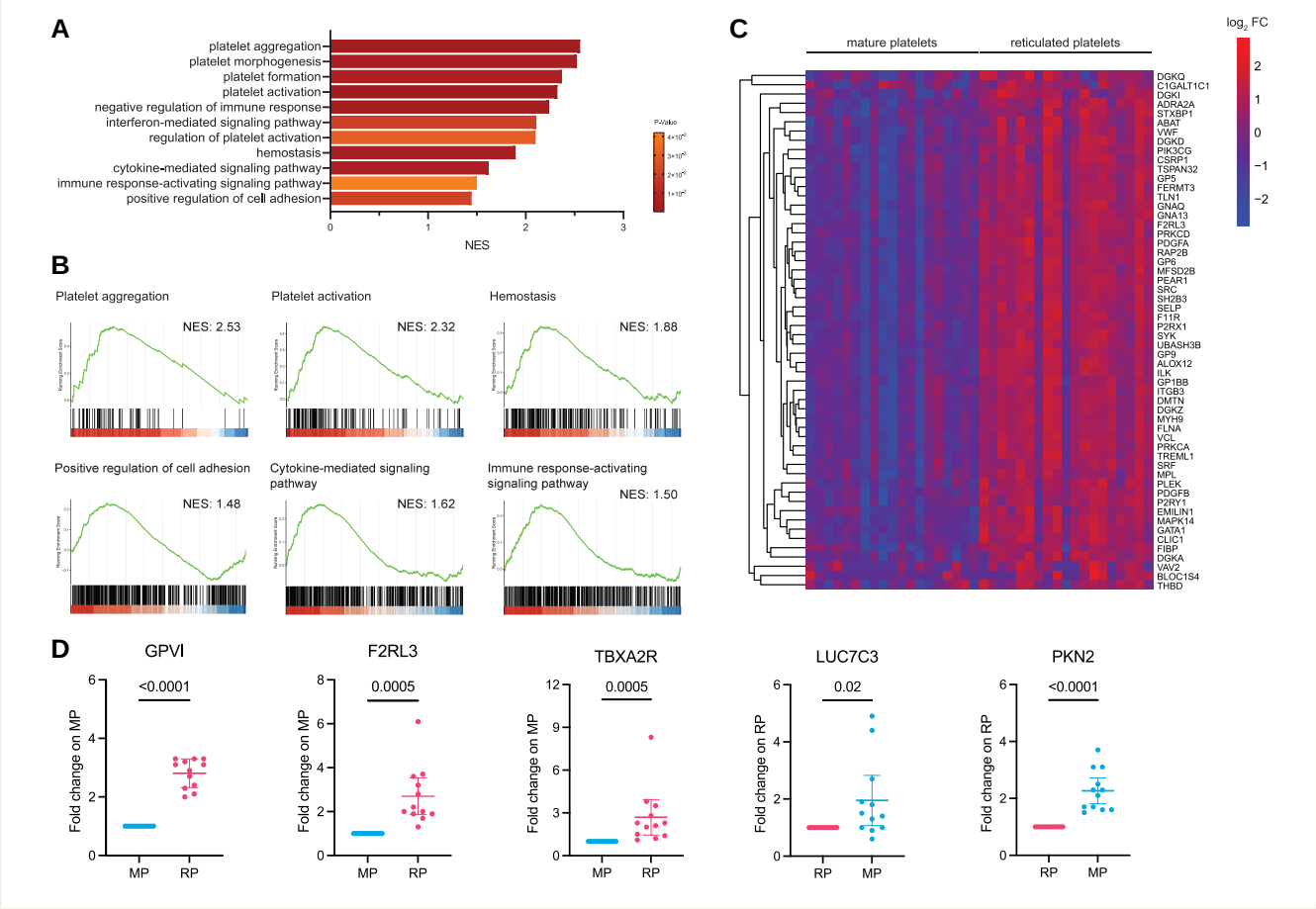

Figure 3 Gene set enrichment analysis (GSEA) of RPs compared to MPs. (*A*) GSEA across the entire transcriptome revealed enrichment of categories related to platelet activation and cell adhesion in RPs. Bars represent the normalized enrichment score (NES), with colour intensity proportional to the log 10 of the *P*-value. (*B*) GSEA plots showing the enrichment scores of six selected relevant gene sets for RPs, with the NES and *P*-value specified for each plot. (*C*) Heatmap displaying leading-edge genes identified by GSEA. Each row represents the relative expression of a single gene across the 19 patients, with expression levels shown as a gradient from low to high ($N = 19$). (*D*) Transcriptome analysis validation by droplet digital PCR. $N = 12$. F2RL3, Protease-activated receptor 4 (PAR-4); GSEA, gene set enrichment analysis; LUC7C3, LUC7 like 3 pre-mRNA splicing factor; MPs, mature platelets; NES, normalized enrichment score; RPs, reticulated platelets

CD62P (P-Selectin) and CD63, as well as collagen receptor GPVI and thrombin receptor PAR1, in both quiescent and stimulated states without data normalization (*Figure 6D*). Western blot analysis of sorted RPs and MPs validated GPVI upregulation in RPs (see Supplementary data online, *Figure S11*).

To account for cell size, normalization was performed using the CD42b signal as previously described,[47] activation markers such as CD62P [median difference 0.23 MSI (95% CI .07, .55)] and CD63 [median difference 0.34 MSI (95% CI .26, .53)] remained significantly up-regulated in RPs (see Supplementary data online, *Figure S12A*, *Tables S18* and *S19*). Additionally, markers such as CD31, CD40, CD41, CD47, CD61, CD69, PAR1, and PEAR1 also showed persistent upregulation.

To account for differences in RNA content, normalization was performed using the iridium-193 signal, which binds RNA. Following this adjustment, markers including CD40, CD62P, CD63, PAR1, and PEAR1 remained significantly up-regulated (see Supplementary data online, *Figure S12B*, *Tables S18* and *S19*). After stimulation with TRAP, RPs consistently showed higher expression of platelet activation markers and transmembrane receptors (see Supplementary data online, *Figure S13*).

When comparing the non-normalized, cell size-normalized, and RNA-normalised datasets, the overall trends and key findings were consistent across all approaches. To further ensure robustness of the paired analyses, we repeated the comparisons using both the paired Wilcoxon signed-rank test and the paired sign test to account for potential skewness in the paired differences (see Supplementary data online, *Table S18*). These sub-analyses revealed minor discrepancies for only two markers after normalization (CD62P and CD36), which did not alter the overall results.

PI3K and GPVI signalling in RPs

The upregulation of receptors PAR1, GPVI, and Integrin β-1 (CD29) in RPs was associated with increased activity in their downstream PI3K signalling pathway (*Figure 7A*). RPs displayed significantly higher levels at FACS of phosphorylated AKT1/2/3, a direct target of PI3K, compared to MPs, both at baseline and following TRAP stimulation

Downloaded from https://academic.oup.com/eurheartj/advance-article/doi/10.1093/eurheartj/ehaf694/8244414 by guest on 09 November 2025

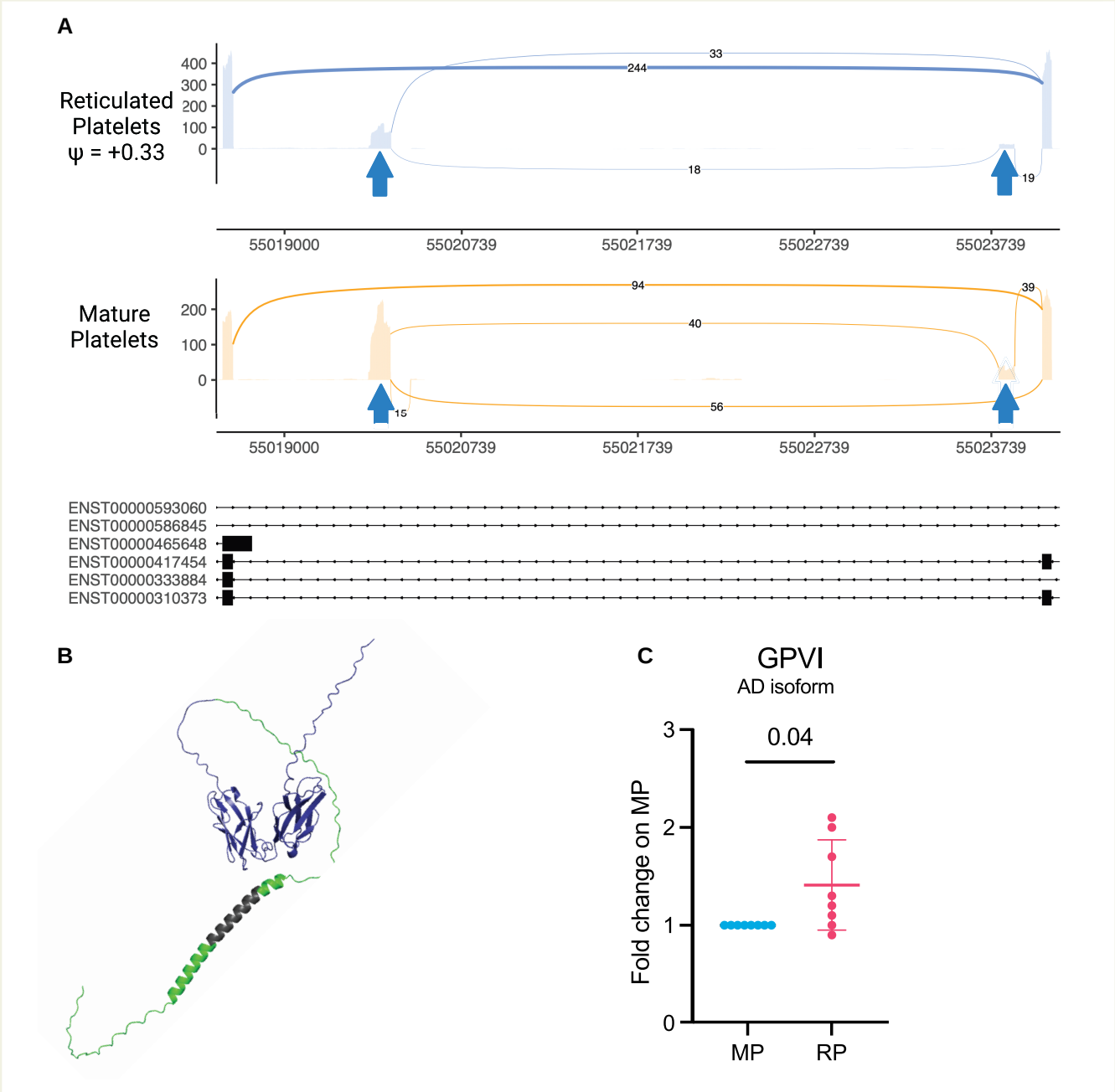

Figure 4 Alternative splicing events of glycoprotein VI (*GPVI*). (*A*) Sashimi plot of *GPVI* alternative splicing events. The exons involved in the novel splicing event are marked with arrows. The isoform lacking these exons is significantly increased in RPs ($\Psi = +0.33$). (*B*) Predicted 3D structure of the canonical *GPVI* isoform (comprising 339 amino acids), obtained from AlphaFold database version 2. Amino acids shared by both the canonical *GPVI* isoform and the two novel *GPVI* isoforms (amino acids 1 to 221) are shown in blue. The region absents in the two novel isoforms (amino acids 222 to 339) is highlighted in green, with the predicted transmembrane helices (amino acids 268 to 287) marked in black ($N = 19$). (*C*) Transcriptome analysis validation of the AD isoform of GPVI by droplet digital PCR ($N = 8$). PCR, polymerase chain reaction; RPs, reticulated platelets

(*Figure 7B*, Supplementary data online, *Figure S14*). Additionally, ROS production, another downstream effect of PI3K activation, was significantly higher in RPs compared to MPs under both baseline and TRAP-activated conditions (*Figure 7C* and Supplementary data online, *Figure S14*).

To further evaluate this pathway, we investigated its inhibition using LY294002. The IC25 and IC95 values for PI3K inhibition, based on normalized P-selectin expression, were determined to be 12.3 and 703 μM, respectively (see Supplementary data online, *Figure S14*). Complete PI3K inhibition at the IC95 concentration effectively suppressed platelet reactivity (see Supplementary data online, *Figure S14*). In contrast, partial inhibition at the IC25 concentration significantly reduced AKT1/2/3 phosphorylation and ROS production in RPs, in baseline and TRAP-activated conditions, while preserving overall platelet reactivity (*Figure 7B* and *C*; Supplementary data online, *Figure S14*). Furthermore, LY294002 treatment at the IC25 level significantly

Downloaded from https://academic.oup.com/eurheartj/advance-article/doi/10.1093/eurheartj/ehaf694/8244414 by guest on 09 November 2025

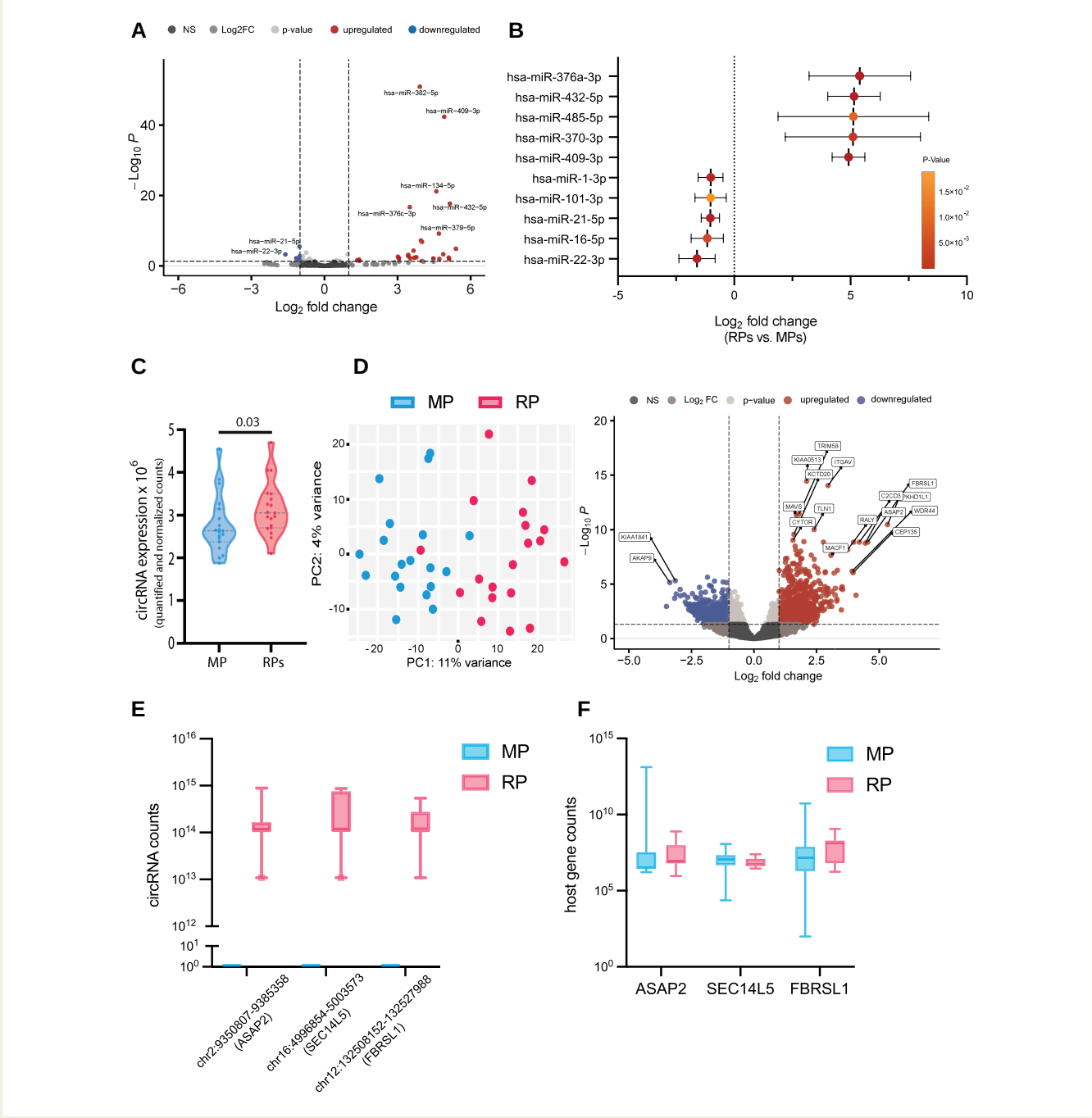

Figure 5 micro and circular RNAs in RPs and MPs. (*A*) Identification of prothrombotic miRNAs in RPs. Volcano plot showing in RPs significantly up-regulated (right) and down-regulated (left) miRNAs. Significant up-/downregulation at $\log_2$ fold change ≥ 1 and *P* value ≤ .05. (*B*) Five most up-/down-regulated miRNA. Colour range is proportional to the log 10 of the *P*-value. (*C*) circRNA expression in RPs and MPs. Expression is shown in quantified and normalised counts in 10^6. (*D*) Left: Principal component analysis (PCA) showing a clustering of RPs and MPs circRNAs. Right: Identification of circRNAs in RPs. Volcano plot showing in RPs significantly up-regulated (right) and down-regulated (left) circRNAs. Significant up-/downregulation at log2 fold change ≥1 and *P* value ≤ .05. (*E*) circRNA counts of RPs specific circRNAs. MPs show only artificial pseudocounts for normalizations to avoid divisions by zero (*F*) Host gene expression counts of RPs specific circRNAs ($N = 19$). MPs, mature platelets; RPs, reticulated platelets

decreased RPs hyperreactivity lowering the expression of P-selectin following TRAP activation (*Figure 7D*). To strengthen these findings, we investigated direct GPVI inhibition using glenzocimab. Treatment with glenzocimab significantly reduced collagen (CRP)-induced RP reactivity, as evidenced by decreased P-selectin expression following CRP activation (*Figure 7E*). A further validation with phospho-signalling profiling using mass cytometry revealed consistently higher levels of pPI3K, pAKT, and pSYK in RPs compared to MPs, confirming enhanced

Downloaded from https://academic.oup.com/eurheartj/advance-article/doi/10.1093/eurheartj/ehaf694/8244414 by guest on 09 November 2025

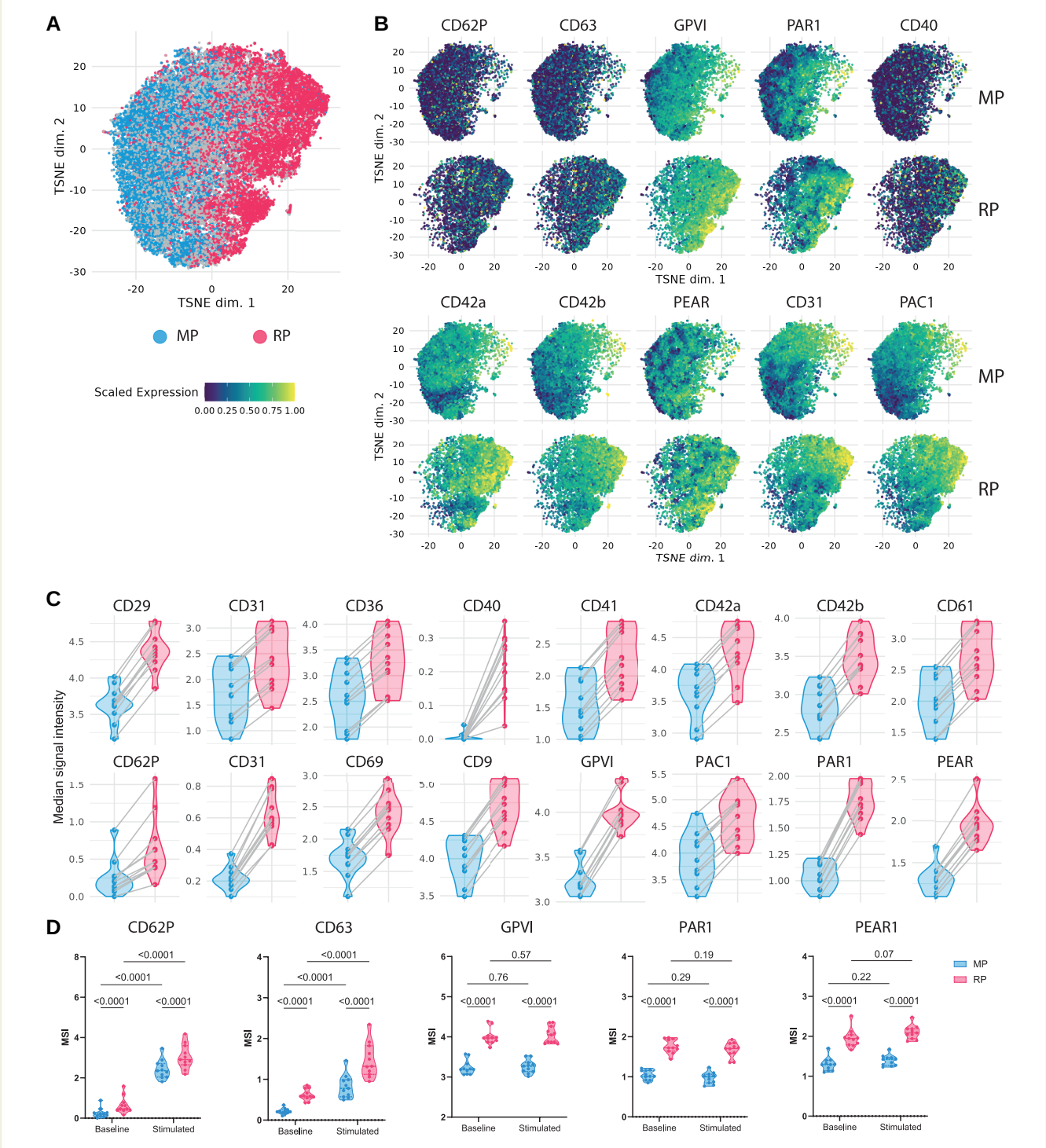

Figure 6 Receptor expression in non-stimulated platelets. (*A*) UMAP representation of platelets of CAD patients, clustering in MPs and RPs subpopulations. (*B*) UMAP of RPs and MPs of CAD patients after equal random sampling from each sample and scaled, arcsinh-transformed expression [0–1] for activation markers and transmembrane receptors coloured according to the expression level. (*C*) Median signal intensity of relevant constitutive transmembrane receptors and activation markers in non-stimulated platelets of CAD patients in MPs (blue) and RPs (red) subpopulations. (*D*) Median signal intensity of relevant constitutive transmembrane receptors and activation markers in non-stimulated and TRAP-stimulated platelets of CAD patients in MPs (blue) and RPs (red) subpopulations ($N = 11$). CAD, coronary artery disease; MPs, mature platelets; RPs, reticulated platelets; UMAP, uniform manifold approximation and projection

Downloaded from https://academic.oup.com/eurheartj/advance-article/doi/10.1093/eurheartj/ehaf694/8244414 by guest on 09 November 2025

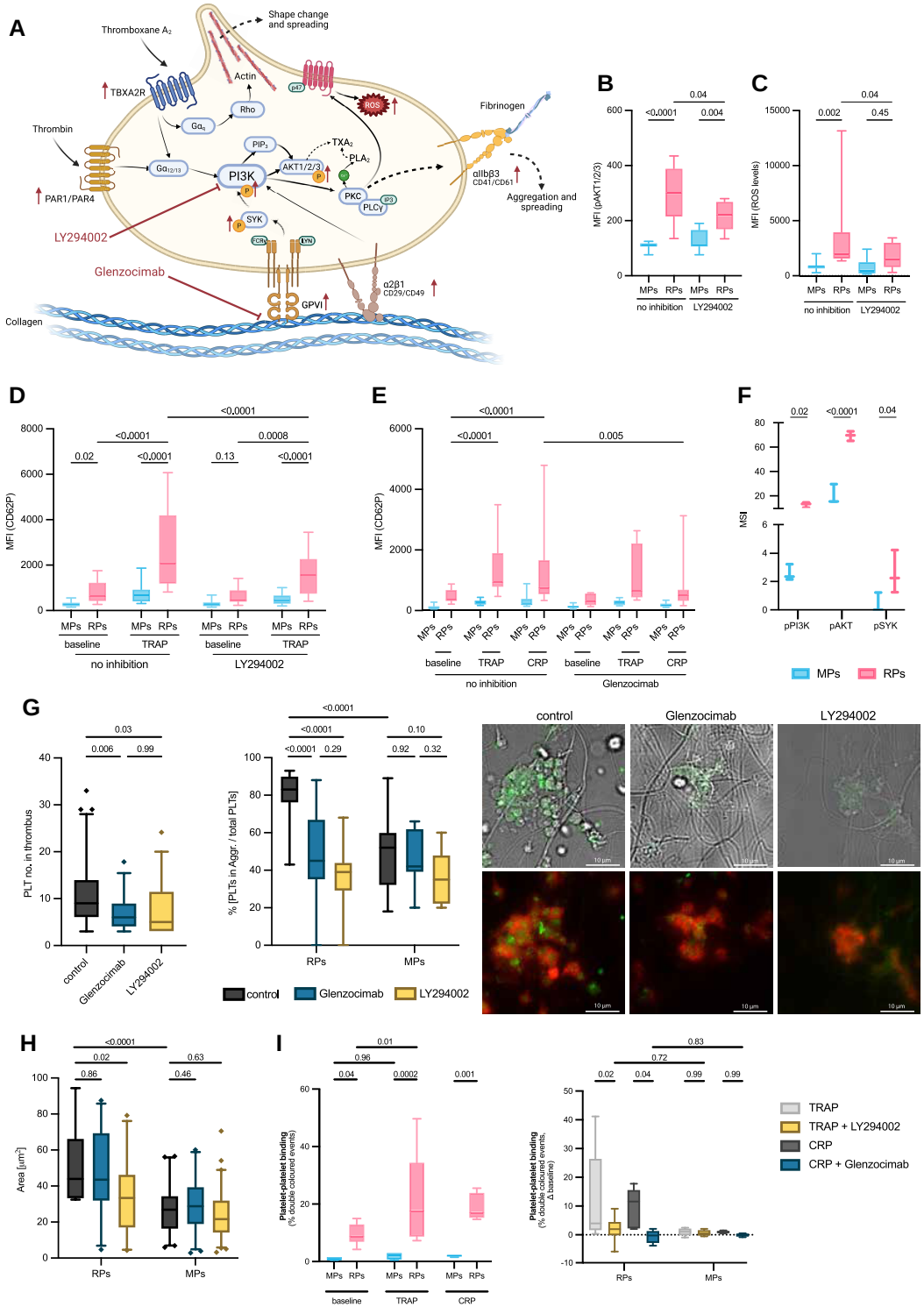

Figure 7 Functional and signalling validation of PI3K and GPVI pathways in RPs and their pharmacological inhibition with LY294002 and glenzocimab. (*A*) Schematic overview of key signalling pathways involving GPVI and PI3K and their downstream effectors. Created with and adapted from Biorender.com (*B*) Phosphorylation of AKT1/2/3 was assessed at baseline with and without LY294002 inhibition (12.3 µM) ($N = 11$). (*C*) ROS production at baseline with and without LY294002 inhibition (12.3 µM) ($N = 11$). (*D*) PI3K inhibition by LY294002. CD62P expression of MPs and RPs after TRAP (10 µM) and inhibition with LY294002 (12.3 µM) ($N = 11$). (*E*) GPVI inhibition by glenzocimab. CD62P expression of MPs and RPs after TRAP (10 µM) and CRP (20 µg/ml) with and without inhibition with glenzocimab (10 µg/ml) ($N = 11$). (*F*) RPs exhibit enhanced phosphorylation of PI3K, AKT, and SYK signalling components. Phosphorylation of key components within the GPVI and PI3K signalling axes were assessed in RPs and MPs using intracellular mass cytometry (CyTOF). RPs demonstrated consistently higher levels of phosphorylated PI3K (pPI3K), AKT (pAKT), and SYK (pSYK) compared to MPs, both

Continued

Downloaded from https://academic.oup.com/eurheartj/advance-article/doi/10.1093/eurheartj/ehaf694/8244414 by guest on 09 November 2025

activation of the GPVI and PI3K signalling axes in RPs (*Figure 7F* and Supplementary data online, *Figure S14*).

Functional validation

To examine platelet behaviour in prothrombotic contexts, we implemented a flow-based chamber assay for *in vitro* thrombosis using collagen and a static fibrinogen-based spreading assay. Under flow, RPs demonstrated significantly greater incorporation into thrombi compared to MPs (*Figure 7G*). Rescue experiments using LY294002 to inhibit PI3K and glenzocimab to inhibit GPVI significantly mitigated these differences, normalizing thrombus composition to MP levels (*Figure 7G*).

Similarly, in fibrinogen-based spreading assays, RPs exhibited enhanced spreading area (*Figure 7H*), which was reversed by LY294002, but not glenzocimab, reinforcing the central role of PI3K signalling in RP-driven platelet activation in prothrombotic conditions.

Flow cytometry-based platelet–platelet binding showed that RPs display a significantly greater increase in platelet–platelet binding compared to MPs upon stimulation with TRAP [mean difference 19.83% double positive events (95% CI 11.38, 28.28), $P = .0002$] and CRP [mean difference 17.63% double positive events (95% CI 8.39, 26.86), $P = .001$]. Rescue experiments with LY294002 and glenzocimab significantly reduced platelet–platelet binding in RPs, to levels comparable to MPs (*Figure 7I*).

Discussion

We present the largest comprehensive investigation of the biology of RPs in CAD patients. The main findings of this study are the following: (i) the hyperreactive RPs are characterized by a prothrombotic transcriptome, with up-regulated transcripts encoding key regulators of platelet activation and function; (ii) RPs have a distinct non-coding signature, including differential regulation of several circRNAs; (iii) the prothrombotic features of RPs are maintained at the proteomic level, with upregulation of key transmembrane proteins, including the collagen receptor GPVI and the thrombin receptors PAR1, leading to an upregulation of the PI3K-mediated pathway; and (iv) PI3K inhibition with LY294002 as well as GPVI inhibition reduced these effects and mitigated RP hyperreactivity, highlighting their potential as therapeutic targets. While prior investigations have offered preliminary insights into RP biology, often in small or healthy cohorts,[12,37] our study provides the first integrated, mechanistic characterization of RPs in patients with CAD. By combining transcriptomics, proteomics, and functional validation, we demonstrate that the hyperreactive phenotype of RPs is driven by specific molecular pathways, notably PI3K-AKT signalling and GPVI-mediated activation. These findings go beyond descriptive profiling by identifying targetable mechanisms that may inform future precision antiplatelet strategies for high-risk CAD patients.

Our results in CAD patients are consistent with early findings in healthy donors, where a similar enrichment of prothrombotic transcripts was observed in RPs.[37] However, a detailed comparison of transcriptomic profiles between healthy donors and CAD patients is beyond the scope of this manuscript. Using high-resolution paired-end RNA sequencing, we detected in CAD patient's upregulation of adhesion proteins, transmembrane receptors, entire activation pathways, and downstream targets such as AKT1 (*Figure 3*).

Small RNA sequencing identified a limited number of miRNAs upregulated in RPs, including miR-432, miR-134, and miR-409, all previously linked to a prothrombotic phenotype. Additionally, alternative splicing analysis uncovered novel events in RPs (see Supplementary data online, *Table S15*), particularly in GPVI transcripts, including two novel exons absent from current genome annotations (*Figure 4*), warranting further study to determine whether these transcripts are coding and to investigate their functional implications.

Our backsplicing analysis revealed the presence of circRNAs, a non-coding RNA class particularly relevant in anucleate cells.[48] RPs exhibited a higher number and significant upregulation of several circRNAs. Notably, we identified three circRNAs uniquely up-regulated in RPs, even though their mRNA precursors were present in both RPs and MPs.

The elevated circRNA levels in RPs were unexpected, given previous reports of circRNA enrichment in platelets during ageing.[48] Our data suggest that hyperreactive RPs are not merely immature platelets but a distinct RNA-rich subpopulation, potentially extending beyond platelet maturation and ageing.[22] Importantly, our transcriptomic analysis was normalized to RNA concentration, transcript length and sequencing depth as well as read counts, accounting for the higher total RNA levels in RPs.

The downregulation of transcripts related to RNA processing in RPs suggests that RNA degradation during maturation does not fully explain our observations. Although further evidence is needed, our data support the idea that RPs represent a more complex heterogeneity, partially pre-programmed during thrombocytopoiesis.[18] Nevertheless, a recent study has demonstrated that platelets undergo age-related phenotypic shifts, transitioning from a prothrombotic profile in

Figure 7 Continued
at baseline and following stimulation with TRAP (10 μM) or CRP (20 μg/ml, shown in Supplementary data online, *Figure S14*). Data are presented as mean signal intensity ($N = 3$ patients; mean ± SD). (*G*) *In vitro* thrombus formation assay: SYTO13 stained PRP was perfused over collagen-coated flow chambers. Quantification of total platelet number in thrombi demonstrated a significant reduction following treatment with glenzocimab (10 μg/ml) or LY2940002 (12.3 μM) ($N = 5$ patients). Stratified analysis revealed that RP incorporation into thrombi was significantly attenuated by both inhibitors, whereas MP incorporation remained largely unaffected. ($N = 5$ patients, $n = 3$ replicates per condition). Representative phase contrast and fluorescent confocal images depict thrombi composed of RPs (SYTO13+/CD41+) and MPs (SYTO13−/CD41+) under control and inhibitor-treated conditions, scale bar (10 μm). (*H*) Platelet spreading assay: SYTO13 stained PRP was incubated on fibrinogen-coated slides. Stratified analysis demonstrated that RP spreading was significantly attenuated by LY2940002 (12.3 μM), but not glenzocimab (10 μg/ml), whereas MP spreading was largely unaffected ($N = 3$ patients, $n = 2$ replicates per condition). (*I*) Flow cytometry-based platelet–platelet binding assay reveals enhanced platelet–platelet binding in RPs and its attenuation by PI3K and GPVI inhibition. Percentage of platelet–platelet binding (defined as double-labelled CD41-BV21+/CD41-APC+ events) at baseline, after TRAP (10 μM) stimulation, and after CRP (20 μg/ml) stimulation in RPs and MPs ($N \geq 5$ patients). Baseline-corrected (Δ baseline) for each condition, showing the change in percentage of platelet–platelet binding after stimulation with TRAP and CRP, or simulation in the presence of the inhibitor, LY294002 (12.3 μM) and glenzocimab (10 μg/ml), relative to baseline or inhibitor-only control conditions. CD62P, P-Selectin; MFI, mean fluorescence intensity; MPs, mature platelets; RPs, reticulated platelets; ROS, reactive oxygen species; TRAP, thrombin receptor activation peptide

Downloaded from https://academic.oup.com/eurheartj/advance-article/doi/10.1093/eurheartj/ehaf694/8244414 by guest on 09 November 2025

younger platelets to an immunomodulatory role in older platelets.[49] While these findings align with our observations of hyperreactive RPs, they also highlight the influence of aging on platelet heterogeneity. Further *in vivo* studies are needed to dissect the contributions of platelet age vs intrinsic programming. However, current models lack the resolution to selectively track RNA-rich platelets *in vivo*, warranting additional experimental elaborations.

Proteomic analysis is essential in CAD, where acute events are driven by protein interactions. We used mass cytometry, adapted for platelet biology through custom antibody conjugation,[39,50,51] to characterize protein expression in RPs. This revealed a differentiation gradient, with higher levels of key receptors and adhesion proteins, including GPVI and PAR1, in RPs compared to MPs. To account for platelet size, we normalized expression using CD42b, as established in flow cytometry.[47] Despite this, activation markers (CD62P, CD63) and transmembrane proteins (PAR1, PEAR1) remained up-regulated in RPs and similar results were observed after normalization for RNA content using iridium (see Supplementary data online, *Table S18*). These differences suggest intrinsic biological programming, potentially reflecting selective cargo transfer from megakaryocytes, a hypothesis that warrants further investigation.[18] Integrating transcriptomic and proteomic data demonstrated consistent upregulation of key platelet receptors and activation markers in RPs, despite expected differences in mRNA and protein levels (see Supplementary data online, *Figure S15*). Notably, while PAR4 was elevated at the RNA level, PAR1 was increased at the protein level, underscoring the complexity of translational regulation and reinforcing the potential relevance of targeting PAR1 in CAD.

Patients with elevated RPs are at heightened risk of ischaemic events despite optimal antiplatelet therapy[34–36]. Notably, our recent meta-analysis demonstrated that elevated RPs are particularly associated with increased risk of cardiovascular death, while associations with myocardial infarction and stroke did not reach statistical significance, likely reflecting low event rates and high heterogeneity.[35] However, the therapeutic potential of RPs has remained speculative due to limited biological characterization. This study addresses this gap by integrating transcriptomic and proteomic analyses, identifying key dysregulated transmembrane proteins in RPs that converge on the PI3K pathway (*Figure 7A*). Indeed, higher phosphorylation of PI3K targets (AKT1/2/3) and elevated ROS levels were observed in RPs, indicating hyperactivity of this pathway (*Figure 7B* and *C*). The hyperactivity of this pathway in RPs may offer a new therapeutic angle to specifically inhibit RPs in CAD patients with elevated RPs. Although it goes beyond the goal of this study to validate a new therapeutic approach, as a proof of principle, we performed an *ex vivo* inhibition of PI3K in platelets of CAD patients. Inhibition of PI3K by IC25 LY294002 significantly reduced RPs hyperreactivity, aggregability, participation in thrombus formation and spreading capacity. Notably, this approach did not completely inhibit platelet reactivity, as platelets were still able to respond to physiological stimuli (*Figure 7D*). Future studies are required to evaluate whether PI3K inhibition could serve as a tailored therapeutic strategy for high-risk patients with elevated RPs. Given the ubiquitous expression of PI3K, targeting alternative proteins in this pathway, for example the collagen-GPVI signalling antagonist revacept, which binds to collagen and prevents its interaction with GPVI and has been recently investigated in a phase II trial, may offer a more specific and clinically viable alternative.[52] However, as revacept requires *in vivo* conditions to exert its effect by binding to collagen, it was not feasible for *ex vivo* experiments, particularly at FACS and mass cytometry. Instead, rescue experiments using glenzocimab, an anti-GPVI Fab, demonstrated a significant reduction in RP reactivity and prothrombotic phenotype following collagen activation, while maintaining the ability of platelets to respond to physiological stimuli (*Figure 7E, G,* and *I*). These findings support the concept that GPVI signalling is particularly relevant in the hyperreactive RP subpopulation. This opens the possibility for stratified, biomarker-guided use of GPVI-targeted therapies in high-risk CAD patients who may not sufficiently benefit from standard antiplatelet regimens. Of note, most patients in our study were on dual antiplatelet therapy, reflecting the high prevalence of recent PCI. The persistence of RP hyperreactivity under these conditions, and its reduction upon GPVI or PI3K inhibition, underscores the potential of these pathways as adjunctive therapeutic targets in high-risk patients. Importantly, our findings align with previous work,[53] which demonstrated that PI3K signalling can be activated under disturbed flow, a common feature in CAD. In our *in vitro* thrombosis assays, RPs showed a higher recruitment into thrombi under flow conditions, which was mitigated by PI3K or GPVI inhibition, supporting the relevance of these pathways.

Finally, to make our data widely accessible, we developed *Platlas* (https://exbio.wzw.tum.de/platlas), an interactive web tool that enables users to navigate, analyse, and stratify our transcriptomic dataset, facilitating further investigations into RP biology and platelet heterogeneity.

Our study has several limitations. First, platelets are challenging to study due to their tendency to activate and aggregate, and their low RNA content complicates analysis. However, we developed and validated experimental pipelines to maintain cell viability and minimize activation during sorting.[13,37] Additionally, we validated a subset of transcriptomic findings in an independent cohort, confirming the robustness of our *in-silico* results (*Figs 3D* and *4C*). Second, while the CAD patients included in this study exhibited heterogeneous baseline characteristics (*Table 1*), including a high prevalence of prior MI and PCI, we specifically designed our study to mitigate inter-individual variability. RPs and MPs were isolated from the same individuals and compared in a pairwise fashion. This intra-patient approach ensures that each subject serves as their own control, thereby eliminating confounding by clinical characteristics or ongoing therapy. As a result, the observed differences between RPs and MPs reflect intrinsic biological features rather than inter-patient variability.

Additionally, while light transmission aggregometry remains a gold standard for platelet function testing, its application was not feasible in our setting due to the limited platelet yield after sorting. We addressed this constraint by employing a validated flow cytometry-based platelet–platelet binding assay, enabling functional characterization of RPs and MPs at single-cell resolution without requiring platelet concentration adjustment.

Intracellular CyTOF revealed higher expression of phosphorylated PI3K, AKT, and SYK (*Figure 7F*); however, it is not possible to determine whether this reflects a generally higher abundance of these proteins in RPs or an inherently higher phosphorylation rate, representing a limitation of the assay.

Finally, the absence of a specific marker for RPs necessitated their definition based on RNA signal intensity (see Supplementary data online, *Figure S16*), as described in prior studies.[13,37,54] While this approach is widely used, the lack of a definitive cutoff impacts the precision of cell sorting and purity. Moreover, although we cannot exclude that TO and iridium signals might partly originate from platelet granules or other subcellular structures, this is a recognized limitation in the field.

In conclusion, this study provides a comprehensive analysis of RP biology in CAD, detailing their distinct prothrombotic features and specific non-coding RNA signatures with unprecedented precision. By uncovering the molecular mechanisms driving RP hyperreactivity,

Downloaded from https://academic.oup.com/eurheartj/advance-article/doi/10.1093/eurheartj/ehaf694/8244414 by guest on 09 November 2025

including the central role of PI3K signalling, we present the first robust mechanistic explanation for their contribution to thrombotic risk. Furthermore, these findings highlight a promising avenue for precision medicine, identifying the inhibition of GPVI and PI3K pathways as a potential strategy to tailor antiplatelet therapy for CAD patients with elevated RPs.

Supplementary data

Supplementary data are available at *European Heart Journal* online.

Declarations

Disclosure of Interest

Z.L. has been an employee of Illumina, Inc. since September 2022. All other authors declare no conflict of interest related to the manuscript.

Data Availability

RNA-seq and mass cytometry data have been made publicly available. RNA sequencing data are available at EGA (https://ega-archive.org/) under access number: EGAD50000001252. Mass cytometry data are available at FlowRepository (flowrepository.org), repository ID FR-FCM-Z8BZ. The code for the transcriptomic analysis and CyTOF post-processing and differential expression analysis is available at https://github.com/daisybio/RPs_MPs and the code for the R Shiny Platlas App is available at https://github.com/daisybio/platlas.

Funding

K.K. was supported by the Studienstiftung des deutschen Volkes. M.H was supported by the Institute for Advanced Study (Technische Universität München), funded by the Deutsche Forschungsgemeinschaft (DFG, German Research Foundation) German Universities Excellence Initiative. Partial support was provided by the Intramural Research Programs (IRPs) of the National Institute of Diabetes and Digestive and Kidney Diseases (NIDDK). Additional funding was received from the Deutsche Forschungsgemeinschaft (DFG, German Research Foundation, grant number 422216132). The work of J.H. was supported by the China Scholarship Council (CSC, grant number 201908370219). D.S. is supported by the DFG (grant SFB1123-B05) and by the DZHK (grant 81Z0600203). The computational infrastructure used in this work was funded by the Deutsche Forschungsgemeinschaft (DFG, German Research Foundation, grant number 422216132). I.B. was supported by Else Kröner-Fresenius-Stiftung (grant number 2020_EKEA.76). D.B. was supported by the Ministero della Salute (Italian Ministry of Health) (Ricerca Finalizzata, GR-2021-12373399), the German Society of Cardiology – Heart and Circulation Research (DGK) Forschungstipendium (DGK102018); Deutsche Stiftung für Herzforschung (grant number F_41_18); Deutsche zentrum für Herz-Kreislaufforschung (DZHK, German Centre for Cardiovascular Research) DZHK Clinician Scientist Programme (grant number 81X3600606); and the Ernst und Berta Grimmke Stiftung.

Ethical Approval

This study was approved by the local ethics committee (Technical University of Munich, Germany Nr 527/18 S-KK and IRCCS Humanitas Research Hospital), and all participants provided written informed consent, and the study was performed in accordance with the Declaration of Helsinki.

Pre-registered Clinical Trial Number

Not applicable.

References

1. Elzey BD, Tian J, Jensen RJ, Swanson AK, Lees JR, Lentz SR, *et al.* Platelet-mediated modulation of adaptive *immunity*. a communication link between innate and adaptive immune compartments. *Immunity* 2003;**19**:9–19. https://doi.org/10.1016/s1074-7613(03)00177-8
2. Maouia A, Rebetz J, Kapur R, Semple JW. The immune nature of platelets revisited. *Transfus Med Rev* 2020;**34**:209–20. https://doi.org/10.1016/j.tmrv.2020.09.005
3. Kapur R, Semple JW. *Platelets* as immune-sensing cells. *Blood Adv* 2016;**1**:10–4. https://doi.org/10.1182/bloodadvances.2016000067
4. Levoux J, Prola A, Lafuste P, Gervais M, Chevallier N, Koumaiha Z, *et al.* Platelets facilitate the wound-healing capability of mesenchymal stem cells by mitochondrial transfer and metabolic reprogramming. *Cell Metab* 2021;**33**:283–99.e9. https://doi.org/10.1016/j.cmet.2020.12.006
5. Nurden AT, Nurden P, Sanchez M, Andia I, Anitua E. Platelets and wound healing. *Front Biosci* 2008;**3525**:3532–48. https://doi.org/10.2741/2947
6. Schlesinger M. Role of platelets and platelet receptors in cancer metastasis. *J Hematol Oncol* 2018;**11**:125. https://doi.org/10.1186/s13045-018-0669-2
7. Thompson CB, Eaton KA, Princiotta SM, Rushin CA, Valeri CR. Size dependent platelet subpopulations: relationship of platelet volume to ultrastructure, enzymatic activity, and function. *Br J Haematol* 1982;**50**:509–19. https://doi.org/10.1111/j.1365-2141.1982.tb01947.x
8. Italiano JE Jr, Richardson JL, Patel-Hett S, Battinelli E, Zaslavsky A, Short S, *et al.* Angiogenesis is regulated by a novel mechanism: pro- and antiangiogenic proteins are organized into separate platelet α granules and differentially released. *Blood* 2008;**111**:1227–33. https://doi.org/10.1182/blood-2007-09-113837
9. van Nispen tot Pannerden H, de Haas F, Geerts W, Posthuma G, van Dijk S, Heijnen HFG. The platelet interior revisited: electron tomography reveals tubular α-granule subtypes. *Blood* 2010;**116**:1147–56. https://doi.org/10.1182/blood-2010-02-268680
10. Bendall SC, Nolan GP, Roederer M, Chattopadhyay PK. A deep profiler's guide to cytometry. *Trends Immunol* 2012;**33**:323–32. https://doi.org/10.1016/j.it.2012.02.010
11. Blair TA, Michelson AD, Frelinger AL III. Mass cytometry reveals distinct platelet subtypes in healthy subjects and novel alterations in surface glycoproteins in glanzmann thrombasthenia. *Sci Rep* 2018;**8**:10300. https://doi.org/10.1038/s41598-018-28211-5
12. Hille L, Lenz M, Vlachos A, Grüning B, Hein L, Neumann F, *et al.* Ultrastructural, transcriptional, and functional differences between human reticulated and non-reticulated platelets. *J Thromb Haemost* 2020;**18**:2034–46. https://doi.org/10.1111/jth.14895
13. Bernlochner I, Klug M, Larasati D, Von Scheidt M, Santovito D, Hristov M, *et al.* Sorting and magnetic-based isolation of reticulated platelets from peripheral blood. *Platelets* 2021;**32**:113–9. https://doi.org/10.1080/09537104.2020.1724923
14. Rodriguez-Martinez A, Simon-Saez I, Perales S, Garrido-Navas C, Russo A, de Miguel-Perez D, *et al.* Exchange of cellular components between platelets and tumor cells: impact on tumor cells behavior. *Theranostics* 2022;**12**:2150–61. https://doi.org/10.7150/thno.64252
15. Gidlöf O, van der Brug M, Öhman J, Gilje P, Olde B, Wahlestedt C, *et al.* Platelets activated during myocardial infarction release functional miRNA, which can be taken up by endothelial cells and regulate ICAM1 expression. *Blood* 2013;**121**:3908–17. https://doi.org/10.1182/blood-2012-10-461798
16. Laffont B, Corduan A, Plé H, Duchez A-C, Cloutier N, Boilard E, *et al.* Activated platelets can deliver mRNA regulatory ago2•microRNA complexes to endothelial cells via microparticles. *Blood* 2013;**122**:253–61. https://doi.org/10.1182/blood-2013-03-492801
17. Koenen RR. Platelets: from simple fragments to inflammation regulators. *Eur Hear J* 2022;**44**:633–5. https://doi.org/10.1093/eurheartj/ehac705
18. Cecchetti L, Tolley ND, Michetti N, Bury L, Weyrich AS, Gresele P. Megakaryocytes differentially sort mRNAs for matrix metalloproteinases and their inhibitors into platelets: a mechanism for regulating synthetic events. *Blood* 2011;**118**:1903–11. https://doi.org/10.1182/blood-2010-12-324517
19. Weyrich AS, Schwertz H, Kraiss LW, Zimmerman GA. Protein synthesis by platelets: historical and new perspectives. *J Thromb Haemost* 2009;**7**:241–6. https://doi.org/10.1111/j.1538-7836.2008.03211.x
20. Healy AM, Pickard MD, Pradhan AD, Wang Y, Chen Z, Croce K, *et al.* Platelet expression profiling and clinical validation of myeloid-related protein-14 as a novel determinant of cardiovascular events. *Circulation* 2006;**113**:2278–84. https://doi.org/10.1161/circulationaha.105.607333
21. Tual-Chalot S, Stellos K. Chrono-pharmacology-based antiplatelet therapy for acute myocardial infarction. *Eur Heart J* 2022;**43**:2335–7. https://doi.org/10.1093/eurheartj/ehac120

Downloaded from https://academic.oup.com/eurheartj/advance-article/doi/10.1093/eurheartj/ehaf694/8244414 by guest on 09 November 2025

22. Bongiovanni D, Han J, Klug M, Kirmes K, Viggiani G, von Scheidt M, *et al.* Role of reticulated platelets in cardiovascular disease. *Arterioscler Thromb Vasc Biol* 2022;**42**:527–39. https://doi.org/10.1161/atvbaha.121.316244
23. Machlus KR, Italiano JE Jr. The incredible journey: from megakaryocyte development to platelet formation. *J Cell Biol* 2013;**201**:785–96. https://doi.org/10.1083/jcb.201304054
24. McBane RD III, Gonzalez C, Hodge DO, Wysokinski WE. Propensity for young reticulated platelet recruitment into arterial thrombi. *J Thromb Thrombolysis* 2014;**37**:148–54. https://doi.org/10.1007/s11239-013-0932-x
25. Armstrong PC, Hoefer T, Knowles RB, Tucker AT, Hayman MA, Ferreira PM, *et al.* Newly formed reticulated platelets undermine pharmacokinetically short-lived antiplatelet therapies. *Arterioscler Thromb Vasc Biol* 2017;**37**:949–56. https://doi.org/10.1161/atvbaha.116.308763
26. Muronoi T, Koyama K, Nunomiya S, Lefor AK, Wada M, Koinuma T, *et al.* Immature platelet fraction predicts coagulopathy-related platelet consumption and mortality in patients with sepsis. *Thromb Res* 2016;**144**:169–75. https://doi.org/10.1016/j.thromres.2016.06.002
27. Hubert RME, Rodrigues MV, Andreguetto BD, Santos TM, de Fátima Pereira Gilberti M, de Castro V, *et al.* Association of the immature platelet fraction with sepsis diagnosis and severity. *Sci Rep* 2015;**5**:8019. https://doi.org/10.1038/srep08019
28. Lakkis N, Dokainish H, Abuzahra M, Tsyboulev V, Jorgensen J, Ponce De Leon A, *et al.* Reticulated platelets in acute coronary syndrome: a marker of platelet activity. *J Am Coll Cardiol* 2004;**44**:2091–3. https://doi.org/10.1016/j.jacc.2004.05.033
29. Perl L, Matatov Y, Koronowski R, Lev EI, Solodky A. Prognostic significance of reticulated platelet levels in diabetic patients with stable coronary artery disease. *Platelets* 2019;**31**:1012–8. https://doi.org/10.1080/09537104.2019.1704712
30. Nardin M, Verdoia M, Negro F, Rolla R, Tonon F, De Luca G. Impact of active smoking on the immature platelet fraction and its relationship with the extent of coronary artery disease. *Eur J Clin Invest* 2019;**50**:e13181. https://doi.org/10.1111/eci.13181
31. Anetsberger A, Blobner M, Haller B, Schmid S, Umgelter K, Hager T, *et al.* Immature platelets as a novel biomarker for adverse cardiovascular events in patients after non-cardiac surgery. *Thromb Haemost* 2017;**117**:1887–95. https://doi.org/10.1160/th16-10-0804
32. Pedersen OB, Larsen SB, Kristensen SD, Hvas A-M, Grove EL. Immature platelets and cardiovascular events in patients with stable coronary artery disease. *Platelets* 2023;**34**:2217960. https://doi.org/10.1080/09537104.2023.2217960
33. Bernlochner I, Goedel A, Plischke C, Schüpke S, Haller B, Schulz C, *et al.* Impact of immature platelets on platelet response to ticagrelor and prasugrel in patients with acute coronary syndrome. *Eur Heart J* 2015;**36**:3202–10. https://doi.org/10.1093/eurheartj/ehv326
34. Bongiovanni D, Schreiner N, Gosetti R, Mayer K, Angiolillo DJ, Sibbing D, *et al.* Immature platelet fraction predicts adverse events in patients with acute coronary syndrome: the ISAR-REACT 5 reticulated platelet substudy. *Arterioscler Thromb Vasc Biol* 2023;**43**:e83–93. https://doi.org/10.1161/atvbaha.122.318614
35. Bongiovanni D, Novelli L, Condello F, Kirmes K, Han J, Wein B, *et al.* Reticulated platelets predict cardiovascular death and adverse events in coronary artery disease: a systematic review and meta-analysis. *Thromb Haemost* 2024;**124**:310–9. https://doi.org/10.1055/s-0043-1773763
36. Elvinger S, Kuehne SG, Patrignani A, Tscharre M, Freynhofer M, Perl L, *et al.* Sex-specific predictive value of reticulated platelets in coronary artery disease: a systematic review and meta-analysis. *Eur J Clin Invest* 2025:e70078. https://doi.org/10.1111/eci.70078.
37. Bongiovanni D, Santamaria G, Klug M, Santovito D, Felicetta A, Hristov M, *et al.* Transcriptome analysis of reticulated platelets reveals a prothrombotic profile. *Thromb Haemost* 2019;**119**:1795–806. https://doi.org/10.1055/s-0039-1695009
38. Banerjee M, Rowley JW, Stubben CJ, Tolley ND, Freson K, Nelson B, *et al.* Prospective, international, multisite comparison of platelet isolation techniques for genome-wide transcriptomics: communication from the SSC of the ISTH. *J Thromb Haemost* 2024;**22**:2922–34. https://doi.org/10.1016/j.jtha.2024.06.017
39. Klug M, Kirmes K, Han J, Lazareva O, Rosenbaum M, Viggiani G, *et al.* Mass cytometry of platelet-rich plasma: a new approach to analyze platelet surface expression and reactivity. *Platelets* 2022;**33**:841–8. https://doi.org/10.1080/09537104.2021.2009453
40. Dowton SB, Beardsley D, Jamison D, Blattner S, Li FP. Studies of a familial platelet disorder. *Blood* 1985;**65**:557–63. https://doi.org/10.1182/blood.V65.3.557.557
41. Daly ME. Transcription factor defects causing platelet disorders. *Blood Rev* 2017;**31**:1–10. https://doi.org/10.1016/j.blre.2016.07.002
42. Krogh A, Larsson B, von Heijne G, Sonnhammer ELL. Predicting transmembrane protein topology with a hidden Markov model: application to complete genomes. *J Mol Biol* 2001;**305**:567–80. https://doi.org/10.1006/jmbi.2000.4315
43. Jumper J, Evans R, Pritzel A, Green T, Figurnov M, Ronneberger O, *et al.* Highly accurate protein structure prediction with AlphaFold. *Nature* 2021;**596**:583–9. https://doi.org/10.1038/s41586-021-03819-2
44. Gao J, Liu J, Zhang Y, Guan B, Qu H, Chai H, *et al.* PBMCs-derived microRNA signature as a prethrombotic status discriminator in stable coronary artery disease. *Thromb Haemost* 2020;**120**:121–31. https://doi.org/10.1055/s-0039-1700518
45. Chen MC, Chang TH, Chang JP, Huang HD, Ho WC, Lin YS, *et al.* Circulating miR-148b-3p and miR-409-3p as biomarkers for heart failure in patients with mitral regurgitation. *Int J Cardiol* 2016;**222**:148–54. https://doi.org/10.1016/j.ijcard.2016.07.179
46. He F, Lv P, Zhao X, Wang X, Ma X, Meng W, *et al.* Predictive value of circulating miR-328 and miR-134 for acute myocardial infarction. *Mol Cell Biochem* 2014;**394**:137–44. https://doi.org/10.1007/s11010-014-2089-0
47. Kanaji T, Ware J, Okamura T, Newman PJ. GPIbα regulates platelet size by controlling the subcellular localization of filamin. *Blood* 2012;**119**:2906–13. https://doi.org/10.1182/blood-2011-08-376566
48. Alhasan AA, Izuogu OG, Al-Balool HH, Steyn JS, Evans A, Colzani M, *et al.* Circular RNA enrichment in platelets is a signature of transcriptome degradation. *Blood* 2016;**127**:e1–11. https://doi.org/10.1182/blood-2015-06-649434
49. Anjum A, Mader M, Mahameed S, Muraly A, Denorme F, Kliem FP, *et al.* Aging platelets shift their hemostatic properties to inflammatory functions. *Blood J* 2025;**145**:1568–82. https://doi.org/10.1182/blood.2024024901
50. Klug M, Lazareva O, Kirmes K, Rosenbaum M, Lukas M, Weidlich S, *et al.* Platelet surface protein expression and reactivity upon TRAP stimulation after BNT162b2 vaccination. *Thromb Haemost* 2022;**122**:1706–11. https://doi.org/10.1055/s-0041-1733934
51. Bongiovanni D, Klug M, Lazareva O, Weidlich S, Biasi M, Ursu S, *et al.* SARS-CoV-2 infection is associated with a pro-thrombotic platelet phenotype. *Cell Death Dis* 2021;**12**:50. https://doi.org/10.1038/s41419-020-03333-9
52. Mayer K, Hein-Rothweiler R, Schüpke S, Janisch M, Bernlochner I, Ndrepepa G, *et al.* Efficacy and safety of revacept, a novel lesion-directed competitive antagonist to platelet glycoprotein VI, in patients undergoing elective percutaneous coronary intervention for stable ischemic heart disease: the randomized, double-blind, placebo-controlled ISAR-PLASTER phase 2 trial. *JAMA Cardiol* 2021;**6**:753–61. https://doi.org/10.1001/jamacardio.2021.0475
53. Selvadurai MV, Moon MJ, Mountford SJ, Ma X, Zheng Z, Jennings IG, *et al.* Disrupting the platelet internal membrane via PI3KC2α inhibition impairs thrombosis independently of canonical platelet activation. *Sci Transl Med* 2020;**12**:eaar8430. https://doi.org/10.1126/scitranslmed.aar8430
54. Hille L, Cederqvist M, Hromek J, Stratz C, Trenk D, Nührenberg TG. Evaluation of an alternative staining method using SYTO 13 to determine reticulated platelets. *Thromb Haemost* 2019;**119**:779–85. https://doi.org/10.1055/s-0039-1681101

Downloaded from https://academic.oup.com/eurheartj/advance-article/doi/10.1093/eurheartj/ehaf694/8244414 by guest on 09 November 2025